

©2018. American Geophysical Union. All Rights Reserved

Access to this work was provided by the University of Maryland, Baltimore County (UMBC) ScholarWorks@UMBC digital repository on the Maryland Shared Open Access (MD-SOAR) platform.

Please provide feedback

Please support the ScholarWorks@UMBC repository by emailing scholarworks-group@umbc.edu and telling us what having access to this work means to you and why it's important to you. Thank you.

JGR Atmospheres

RESEARCH ARTICLE

10.1029/2022JD037473

Key Points:

- The satellite observations exhibit significant correlations and consistent variations and trends with in situ surface measurements
- NO₂ record over Texas show significant decline in populated cities and an increase of up to 80% over oil and natural gas extraction regions
- COVID-19-related restrictions in Texas lead up to a 60% reduction in NO₂ levels that exceed the reduction achieved in the past 15 years

Correspondence to:

M. S. Gyawali and L. N. Lamsal,
madhu.gyawali@sjcd.edu;
lok.lamsal@nasa.gov

Citation:

Gyawali, M. S., Lamsal, L. N., Sedai, J. R., Gyawali, B., Bhattarai, K., Williams, Q., et al. (2023). Tracking NO₂ pollution changes over Texas: Synthesis of in situ and satellite observations. *Journal of Geophysical Research: Atmospheres*, 128, e2022JD037473. <https://doi.org/10.1029/2022JD037473>





Received 11 JUL 2022

Accepted 26 JAN 2023

Author Contributions:

Conceptualization: Madhu S. Gyawali, Lok N. Lamsal, Keshav Bhattarai
Data curation: Jay R. Sedai
Formal analysis: Madhu S. Gyawali, Lok N. Lamsal, Jay R. Sedai, Bimal Gyawali, Keshav Bhattarai, Quintaria Williams, Shannon Neige, Shriram Sharma, Rudra Aryal
Investigation: Madhu S. Gyawali, Lok N. Lamsal, Quintaria Williams, Rudra Aryal
Methodology: Madhu S. Gyawali, Lok N. Lamsal, Keshav Bhattarai, Shriram Sharma
Software: Bimal Gyawali
Validation: Lok N. Lamsal
Visualization: Jay R. Sedai, Bimal Gyawali
Writing – original draft: Madhu S. Gyawali, Lok N. Lamsal, Jay R. Sedai, Bimal Gyawali, Keshav Bhattarai, Shriram Sharma, Rudra Aryal

Tracking NO₂ Pollution Changes Over Texas: Synthesis of In Situ and Satellite Observations

Madhu S. Gyawali¹ , Lok N. Lamsal^{2,3} , Jay R. Sedai⁴, Bimal Gyawali⁵ , Keshav Bhattarai⁶, Quintaria Williams¹, Shannon Neige¹ , Shriram Sharma⁷, and Rudra Aryal⁸

¹Undergraduate Research Center, San Jacinto College, South Campus, Houston, TX, USA, ²Goddard Earth Sciences Technology and Research II, University of Maryland Baltimore County, Baltimore, MD, USA, ³NASA Goddard Space Flight Center, Greenbelt, MD, USA, ⁴Abacus Insights, Boston, MA, USA, ⁵Department of Earth and Atmospheric Science, University of Houston, Houston, TX, USA, ⁶Department of Physical Sciences, University of Central Missouri, Warrensburg, MO, USA, ⁷Department of Physics, Amrit Campus, Tribhuvan University, Kathmandu, Nepal, ⁸Franklin Pierce University, Rindge, NH, USA

Abstract Nitrogen oxides (NO_x) are major air pollutants that play a crucial role in atmospheric chemistry. We compare Ozone Measuring Instrument's (OMI) NO₂ records with the in situ surface measurements from the Air Quality System of the US Environmental Protection Agency and the Texas Commission on Environmental Quality network in the state of Texas with the goal of understanding the correspondence of satellite and in situ surface observations and identifying the potential synergies between the two observing systems. Our analysis of over 40 in situ daily surface site observations, mostly from urban areas, and OMI daily observed data suggests a correlation (*r*) ranging between 0.2 and 0.8. The correlation improves considerably (*r* > 0.5) for monthly average data. Weekly variation of surface NO₂ with a Sunday minimum is well captured by OMI tropospheric NO₂ column observations with similar weekend reductions. NO₂ trend in Texas during 2005–2019 is characterized by significant reductions of 20%–36% in highly populated cities and urban centers. However, a significant (up to 80%) increase was observed in oil and gas producing regions of the Permian and Eagle Ford Basins over the same period. In March–April of 2020, like the other US and global cities, Texas experienced up to 60% reduction in NO₂ levels in major cities due to travel restrictions imposed at local and national levels to contain the spread of COVID-19. Though such reduction is temporary, these reductions were significantly larger than those achieved in the past 16 years of OMI record suggesting that technological advancement can curtail NO_x emissions.

Plain Language Summary Linking satellite and ground-based observations, this study presents variation and long-term trends in Texas's nitrogen dioxide (NO₂) concentration. Nitrogen oxides (NO_x = NO + NO₂) are major air pollutants that play an important role in atmospheric chemistry. We compare NO₂ records from the Ozone Measuring Instrument with the in situ surface measurements from the Air Quality System of the US Environmental Protection Agency and the Texas Commission on Environmental Quality to identify the potential synergies between the two observing systems. Our analysis of 40 surface sites suggests a fair to excellent correlation. NO₂ trend in Texas during 2005–2019 is characterized by significant reductions of 20%–36% in highly populated cities and urban centers. However, over the same period, a substantial increase of up to 80% was observed in oil and gas-producing regions of the Permian and Eagle Ford Basins. Moreover, in March–April of 2020, Texas experienced up to 60% reduction in NO₂ levels in major cities due to travel restrictions imposed at local and national levels to contain the spread of COVID-19. Though such reduction is temporary, these reductions were as significant as those achieved in the past 16 years of OMI, suggesting that technological advancement can curtail NO_x emissions.

1. Introduction

Nitrogen dioxide (NO₂) is one of the six “criteria” air pollutants regulated by the United States Environmental Agency (EPA) (US EPA, 2017). It is a toxic gas and a marker of pollutants created by fuel combustion. Nitrogen oxides (NO_x = nitric oxide (NO) + NO₂) alter the hydroxyl radical (OH) concentration, control the formation of ozone (O₃) (Bradshaw et al., 2000), and contribute to the atmospheric aerosol formation (Crutzen, 1979; Lelieveld et al., 2004), thereby impacting air quality and the earth's radiation budget in the troposphere. NO_x is emitted by anthropogenic activities and natural processes (Bradshaw et al., 2000; Crutzen, 1979; Navarro-González

Writing – review & editing: Lok N. Lamsal, Quintaria Williams, Shannon Neige, Shriram Sharma, Rudra Aryal

et al., 2001); anthropogenic sources include all fuel combustion processes, and natural sources include lightning and soil emissions. Understanding NO_x sources, their evolution, and long-term trends could help mitigate air pollution (Cohen et al., 2017; Mills et al., 2009) without negatively impacting economic activities.

A significant portion of the Texas economy depends on energy production, accounting for 43% of U.S. crude oil and 26% of natural oil gas production in 2020 (US EIA, 2021), and is projected to reach record-high levels in the coming years (US EIA, 2022). Texas has one of the world's largest petrochemical complexes, and it is the largest natural gas-producing state in the US. Previous studies have shown that various emission sources, such as petrochemical manufacturing and refineries, powerplants, motor vehicle exhaust, and biogenic emissions are contributing to a complex mixture of pollutants in the ambient air in Texas (Buzcu-Guven & Fraser, 2008; Caicedo et al., 2019; Jobson et al., 2004; Leuchner & Rappenglück, 2010). Interaction of NO_x emissions from the south and east Texas shale oil regions with relatively large emissions of biogenic hydrocarbons in the region have implications for ozone and air quality problems in many urban metropolitan areas (Kemball-Cook et al., 2010; Pacsi et al., 2015). Increasing emissions from oil refineries and gas industries are of public concerns due to the negative health impact of air pollutants despite their contributions to Texas economy (Bunch et al., 2014; Cushing et al., 2021; Field et al., 2014; Macey et al., 2014). While regular monitoring of air quality has become important for public health for the entire state of Texas, there are observational constraints. We demonstrate here that we can address this issue by complementing in situ surface observations with NO_2 column observations from satellite. Satellite monitoring of NO_2 changes over oil and gas production regions could help inform changes in flaring and emissions of other gases such as methane due to market fluctuation (Lyon et al., 2021; Majid et al., 2017) or changes in maintenance (Laughner et al., 2021).

Often referred to as the Lone Star State, Texas is the second-most populous state in the US and is home to four cities with more than one million people and 42 cities with population greater than 100,000 people (Bureau, 2017). The population size of cities and municipalities is growing due to the steady influx of people. Rapid urbanization and industrialization cause land use and cover changes and contribute to increasing levels of air pollution (Fan et al., 2020; Farmer et al., 2014; Wang et al., 2017). Various regions, including highly populated metropolitan areas in Texas, have been experiencing complex air quality problems, and some parts are declared ozone non-attainment (Byun et al., 2005; Kim et al., 2011; Sourì et al., 2016). The land-sea breezes circulation and wind patterns over coastal areas further complicate pollutants movements deteriorating the air quality (Banta et al., 2005; Caicedo et al., 2019; Chen et al., 2011; Fan et al., 2020; Jacob & Winner, 2009; Nowlan et al., 2018). It is thus necessary to identify and quantify the most significant anthropogenic emissions, such as NO_x , to effectively mitigate air pollution to help improve human health (Demetillo et al., 2020; McDonald et al., 2018).

Recognizing air quality problems in Texas, several studies have been conducted utilizing existing routine measurements as well as measurements made during some dedicated field campaigns, such as Texas Air Quality Study (TexAQS) (Berkowitz et al., 2005; Daum et al., 2003) in 2000 and TexAQS II (Parrish et al., 2009) in 2006, Deriving Information on Surface conditions from Column and Vertically Resolved Observations Relevant to Air Quality (DISCOVER-AQ) (Anderson et al., 2014) in 2014, and TRacking Aerosol Convection interactions Experiment—Air Quality (TRACER-AQ) (Jensen et al., 2021) in 2021. Most prior studies were concerned with emissions of NO_x and hydrocarbons, from industrial complexes and powerplant changes of NO_2 levels over cities (Demetillo et al., 2020; Duncan et al., 2016; Lamsal et al., 2015) and oil and natural gas extraction regions (Majid et al., 2017; Roest & Schade, 2020; Schade & Roest, 2016, 2018) in Texas. Continuous hourly air quality observations, including NO_2 , from the air quality system (AQS) of US Environmental Protection Agency (EPA) and Texas Commission on Environmental Quality (TCEQ) monitoring networks (Schade & Roest, 2016, 2018; Zhang et al., 2018) have been a valuable resource for studying tropospheric composition, air quality, and their linkage to public health. In regard to NO_2 , in particular, there are certain limitations with the use of surface monitoring network data due to its sparse and heterogeneous siting (see Figure 1). In contrast, space-based observations provide better spatial coverage, complementing the existing ground-based in situ measurements, and provide coverage where in situ ground measurements are unavailable (Bechle et al., 2013; van Donkelaar et al., 2006). This study takes advantage of both of these resources with improved NO_2 data quality (Lamsal et al., 2021) from the Ozone Monitoring Instrument (OMI) flying on NASA Aura satellite (Duncan et al., 2016; Lamsal et al., 2008, 2014, 2015; Levelt et al., 2006, 2018; Veefkind et al., 2006). A combination of OMI's Texas-wide early afternoon NO_2 data with EPA AQS' continuous hourly NO_2 observations over the past 16 years will help us to characterize NO_2 variations and trends fully, understand the relationship between NO_2 surface and column density, and also identify the strengths and limitations of the two observing systems.

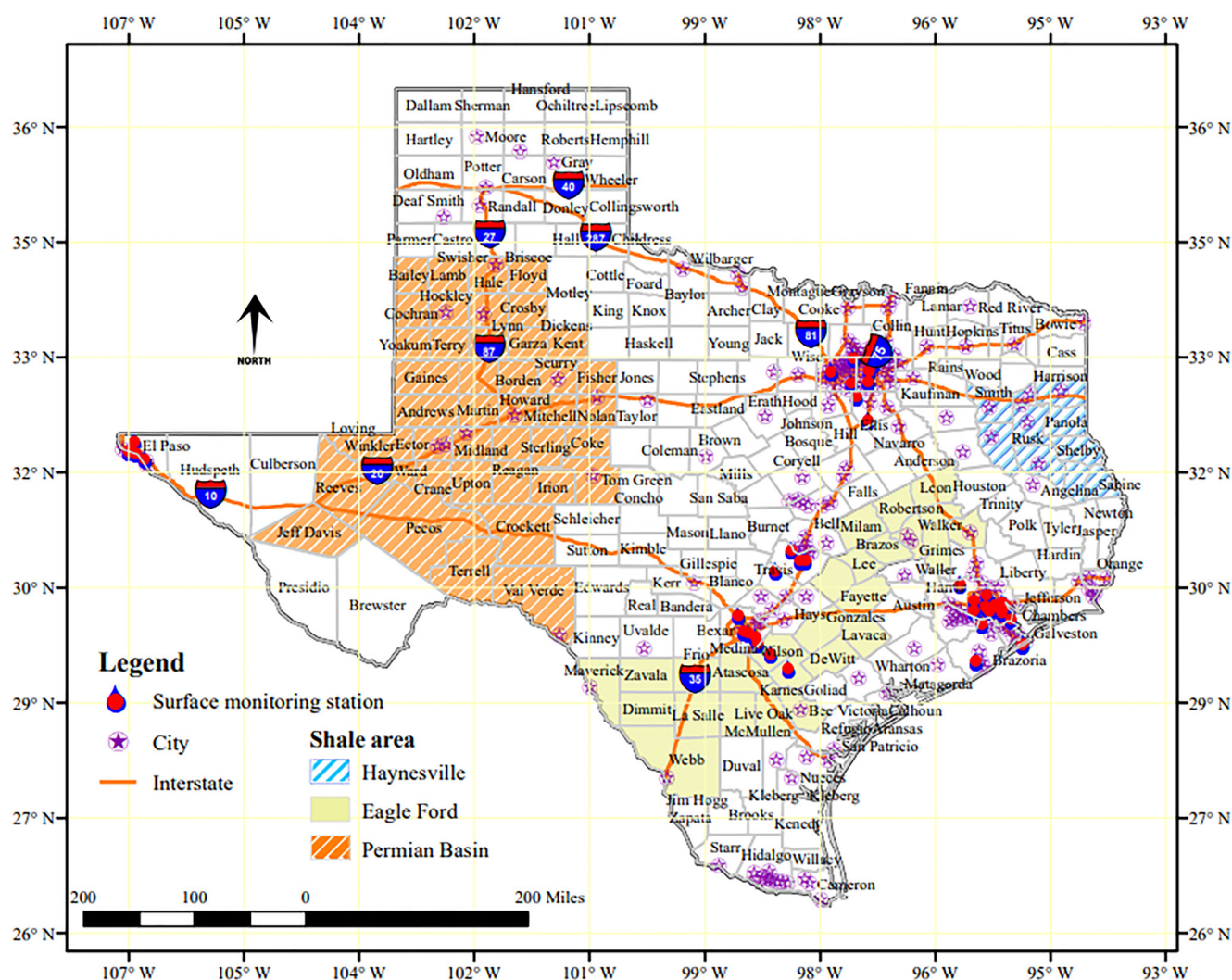


Figure 1. Texas map showing the location of major cities (circled purple stars), three basins (shaded regions), and EPA's and TCEQ's ground monitors (red circles).

The rest of the manuscript is structured as follows: in Section 2, we briefly describe the OMI and surface NO_2 measurements. In Section 3.1, we examine the correspondence between NO_2 surface measurements (from TCEQ and EPA AQS) and OMI satellite NO_2 vertical column observations over several sites in six largest cities in Texas. We elaborate this further examining NO_2 weekly cycles in Section 3.2. In Section 3.3, we examine NO_2 trends for the state of Texas, several large cities, and shale oil regions.

2. Geography, Data and Method Description

2.1. Study Area and Site Locations

Texas is one of the migratory destinations and densely populated states of the United States where the population grew by 20% between 2000 and 2010 and by 16% between 2010 and 2020 (Bureau, 2020). Most of the increase occurred in major cities such as Austin-Round Rock, Dallas-Fort Worth, San Antonio, Houston, and Laredo. The Houston, Galveston, and Brazoria area, which consists of eight counties (Figure 1), was a nonattainment area in the 2008 National Ambient Air Quality Standard (NAAQS) for ozone. Using the Environmental Protection Agency's (EPA's) findings on the status of ozone levels in El Paso County exceeding the 2015 NAAQS (US EPA, 2021), the American Lung Association has reclassified El Paso county as the most smog-polluted metropolitan area (American Lung Association, 2022).

There are over 162,109 oil wells and 84,801 gas wells in the state of Texas as of May 2022 (“Texas Oil and Gas Production Statistics for February 2022,” n.d.). Several high levels of oil and gas producing counties are comprised of Permian Basin, Eagle Ford Shale, and Haynesville that we focus on this study (Figure 1). We exclude the Barnett shale play because of its proximity to Dallas-Fort Worth Metroplex, the fourth largest metropolitan area in the US, as it will be difficult to isolate the contribution of emissions from urban and shale play activities. Permian Basin is one of the largest and oldest oil-producing regions in West Texas bordering New Mexico State in the west. The hydraulic fracturing techniques used for oil production results in enhanced emissions of CH_4 , CO_2 , and NO_x (McKenna, 2020). The Eagle Ford Shale oil region in southern part is black calcareous shale with high organic carbon content. Since 2008, it has been one of the most heavily drilled rock units in the United States and hence has become the dominant regional source of NO_x emissions (Schade & Roest, 2018). The horizontal drilling technology has accelerated the extraction of gases, but at the expense of degraded air quality in 23 counties of Texas. The Haynesville shale region, located in the eastern part of Texas, borders Louisiana, covers 23 counties and has conventional oil and natural gas deposits. EPA updated the NO_2 status in these basins and categorized it as an ozone nonattainment region (Lamsal et al., 2015).

2.2. Data Sources

2.2.1. OMI NO_2 Observations

The Ozone Monitoring Instrument (OMI), launched in 2004 on NASA's Aura satellite, is a nadir viewing spectrometer with a wide field of view (Boersma et al., 2007, 2008; Lamsal et al., 2015; Levelt et al., 2006). OMI flies in a sun-synchronous polar orbit at an altitude of 705 km and crosses the equator at $\sim 13:45$ local time in ascending mode with nearly global coverage every day. Its ground resolution is $13 \times 24 \text{ km}^2$ at nadir, while the resolution can be as large as $26 \times 128 \text{ km}^2$ at swath edges. OMI measures solar and backscatter radiation in the ultraviolet-visible spectral range from 264 to 504 nm at a medium spectral resolution of $\sim 0.6 \text{ nm}$, allowing observation of various trace gases in the atmosphere.

We use the OMI NO_2 standard product, version 4.0 (Lamsal et al., 2021), available from the NASA Goddard Earth Sciences Data Active Archive Center (GES DISC; <http://disc.sci.gsfc.nasa.gov>). The NO_2 retrieval process involves multiple procedures and is mainly based on the differential optical absorption spectroscopy (DOAS) technique (Platt & Stutz, 2008). First, as discussed in Marchenko et al. (2015) and Lamsal et al. (2021) the algorithm utilizes radiance and irradiance measurements in the 402–465 nm spectral range to retrieve the NO_2 slant column densities (SCDs), which represents NO_2 abundance along the viewing path. Second, air mass factors (AMFs) are calculated to convert SCDs into vertical column densities (VCDs) of NO_2 . The final step involves removing cross-track artifacts (or stripes) and separating the tropospheric and stratospheric NO_2 VCD components, as discussed in detail in Bucseles et al. (2013). The most recent version 4.0 NO_2 product has incorporated multiple improvements and updates, especially in the AMF calculation, that lead to an improved agreement of OMI NO_2 products with independent observations (Lamsal et al., 2021).

We use the OMI tropospheric NO_2 VCD data, mapped onto a regular grid of 0.1° latitude \times 0.1° longitude, publicly available from the NASA Aura Validation Data Center website (<https://avdc.gsfc.nasa.gov/pub/data/satellite/Aura/OMI/V03/L3/>). The high-quality pixel-level data with effective cloud fraction < 0.3 and not affected by row anomaly (Dobber et al., 2008) were used to generate this product.

2.2.2. EPA and TCEQ Surface NO_2 Measurements

We use the publicly available in situ surface NO_2 data from the US EPA AQS (https://aqs.epa.gov/aqsweb/airdata/download_files.html) and TCEQ (<https://www17.tceq.texas.gov/tamis/index.cfm>) networks (Demerjian, 2000; Schade & Roest, 2016, 2018). These networks provide long-term NO_2 hourly data for many urban, suburban, and rural areas in the US (Demerjian, 2000; Silvern et al., 2019). The afternoon time (13:00–14:00) data from the two networks are analyzed, matching with OMI observations. The network employs the NO_2 chemiluminescence analyzers equipped primarily with a molybdenum converter to measure ambient NO_2 concentrations, which are known to have high biases due to interfering oxidized nitrogen species such as nitric acid, peroxyacetyl nitrates, and alkyl nitrates (Bechle et al., 2013; Lamsal et al., 2008; Silvern et al., 2019). The bias could vary spatially and temporally and is cumbersome to account for due to the lack of observation of the interfering species. This bias, however, is expected to have a minor impact on seasonal and trend comparisons between OMI and surface measurements discussed here (Lamsal et al., 2015). Therefore, we have not made any attempts here to account for the high bias in surface monitor data.

We use data from 38 EPA AQS sites primarily located in urban areas and 2 TCEQ sites located in rural areas. We focus on sites that cover longer term data after 2005 when OMI started routine measurements. The number of ground monitoring sites varies by cities, with 14 locations in Houston, eight in Dallas, five in El Paso and San Antonio each, four in Austin, and two in Galveston (Figure 1). The sites maintained by TCEQ offer measurements after 2013 only, but they are the only rural sites available (Schade & Roest, 2016, 2018). While the majority of the sites offer continuous long-term measurements, some areas either cease operation or relocated elsewhere. We discuss this further in Section 3.1.

2.3. Trend Analysis

We use the multivariate regression model to analyze the contributions of various factors to the monthly averages of Ozone Monitoring Instrument (OMI) NO₂ data from 2005 to 2019. We follow the analysis method described in Lamsal et al. (2015). This method extracts linear trend term, seasonal component, and noise component from the monthly average of OMI NO₂ data, $Y(t)$, as below:

$$Y(t) = L \times t + S(t) + R(t), \quad (1)$$

where a linear trend component, L , quantifies long-term changes in NO₂; t represents the number of months since January 2005, while $S(t)$ provides the variations of a time-dependent seasonal component; and $R(t)$ describes the residual or noise component that can't be described by the linear trend or the seasonal component. The residual part contains the impact of short-term variations such as transport in NO₂ columns. The time dependent seasonal component, $S(t)$, can further be expressed as a sum of trigonometric series and a constant term:

$$S(t) = \sum_{n=1}^3 \left(a_n \cos\left(\frac{2\pi nt}{12}\right) + b_n \sin\left(\frac{2\pi nt}{12}\right) \right) + c \quad (2)$$

The constant coefficients such as a_n , b_n , and c are the fit parameters. The regular seasonal NO₂ cycle is mostly related to the seasonal variation of the NO_x lifetime; the seasonal amplitude of NO₂ could evolve in time depending upon the magnitude of the NO₂ amount (Lamsal et al., 2015). The changes in amplitude and phase for the specific year can be inferred by fitting a regression line for that year plus 6 months from the given year (i.e., 24 months in total). This process is repeated for each year to determine yearly varying seasonal component. The absolute changes on OMI NO₂ were calculated by applying two least-squares regression models onto the de-seasonalized time series. Any systematic high or low biases in satellite retrievals are unlikely to affect the trend presented here in a major way. The random biases are expected to be minimized with the monthly average data, and are considered in residuals. We perform a t -test with the residuals and determine the statistical significance of the linear trend at 95% confidence. Here we note that this approach of determining the monthly rate of change over a specified period is more appropriate if the pace of change is uniform, and a careful interpretation is needed for non-uniform pace of changes.

3. Results and Discussion

3.1. Correspondence Between OMI and EPA/AQS Observations

This section examines how surface measurements compare with collocated OMI NO₂ column observations spatially and temporally. Over moderately polluted areas, a tropospheric column of 1×10^{15} molec. cm⁻² roughly corresponds to surface NO₂ mixing ratio of 0.5 ppb, but there is no unique relationship as the relationship depends on various factors (e.g., mixing layer depth, amount of NO₂ in the free-troposphere). Therefore, a direct comparison and interpretation is difficult between OMI tropospheric NO₂ VCDs and surface NO₂ mixing ratios. Here we analyze multi-year (2005–2021) NO₂ observations from OMI and surface monitors over 40 sites. The 38 sites are primarily located in six major cities in Texas: Houston, San Antonio, Dallas, Austin, Galveston, and El Paso, while the two sites are located in rural regions in Wilson and Karen counties of the Eagle Ford basin. To compare, we collocate OMI and surface observations in both space and time (13:00–14:00 local time) and analyze cloud-free (effective cloud fraction <30%) and quality-controlled data.

Figure 2 shows the comparison between OMI tropospheric NO₂ VCD and EPA AQS in situ NO₂ mixing ratios over all available ground monitors in six major cities in Texas. The number of samples for each measurement site ranges from a few hundreds to a few thousand. It varies depending on the duration and continuity of operation for

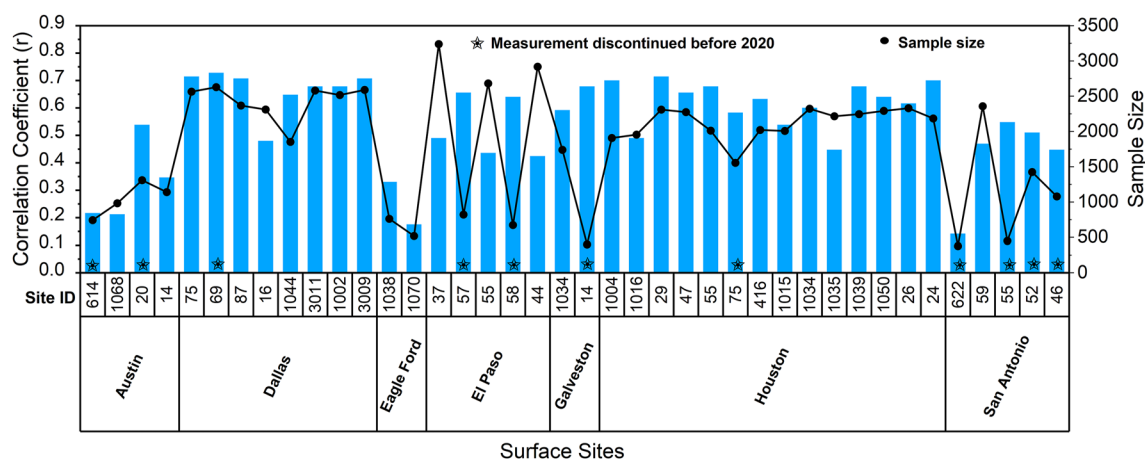


Figure 2. Correlation between collocated OMI tropospheric NO₂ VCDs, and EPA AQS and TCEQ NO₂ mixing ratios over 40 sites in Texas. Blue bars show the correlation coefficient with a total number of collocated samples (black line with circles) shown on the right y-axis. The operation status of the sites is indicated (blue stars). Urban locations and site IDs are noted.

ground monitors and local cloudiness conditions for OMI. For instance, surface sites that discontinued operation appear to have a smaller sample size. The correlation between AQS and OMI calculated from simultaneous daily measurements during 2005–2020 is significant for most sites but varies depending on sample size and monitor locations. The correlations are generally higher for Dallas and Houston, with correlation coefficients varying between 0.4 and 0.8. El Paso and Galveston exhibit similar variations with correlation coefficients ranging from 0.4 to 0.6. Sites in Austin, in general, show somewhat lower correlation coefficients, from 0.2 to 0.5, partly due to smaller sample sizes. Except one site, we observe moderate to high correlation ($r > 0.5$) for sites in San Antonio despite having comparatively fewer samples. The two rural sites in Eagle Ford basin exhibited rather low correlations ($r < 0.3$), likely be due to low NO₂ levels, reduced satellite sensitivity, and increased errors in satellite NO₂ retrievals. The correlation between OMI and surface observations observed in Texas is consistent with many other prior studies in other areas in North America (Cooper et al., 2022; Lamsal et al., 2008). Considering local point measurement of NO₂ mixing ratios by ground monitors and an aerial average of a total number of NO₂ molecules in the troposphere by OMI, the observed relationship between the two observations over polluted areas is noteworthy with significance to observing surface level NO₂ pollution from satellite instruments.

Figure 3 shows monthly time series of area-averaged tropospheric NO₂ VCD from OMI compared with concurrent NO₂ mixing ratios from all EPA ground monitors from the six cities shown in Figure 2. Overall, the time series for 2005–2020 shows that the two measurement systems exhibit similar variations for all cities except for specific events and locations when the active sensors were discontinued, and additional sensors were installed in new areas. This occurred in San Antonio in 2011 and Austin in 2013 as indicated in the shaded regions, Figure 3. For example, the unexpected jump in the AQS surface NO₂ mixing ratios in Austin after 2013 is due to the installation of a new monitor (ID: 1068) closer to Interstate 35. Similarly, the uptick in NO₂ mixing ratios in San Antonio after 2011 resulted from two monitors' discontinuations from relatively clean locations. Aside from these specific scenarios, the correspondence of the long-term OMI tropospheric NO₂ VCD and AQS surface NO₂ concentration measurements is remarkable ($r = 0.78$ for El Paso, 0.83 for Dallas, 0.78 for Houston, 0.79 for Galveston), given that this comparison is between the vertical column versus point NO₂ levels. In addition, both data sets indicate a substantial decrease in NO₂ levels in several major Texas cities, as discussed further in Section 3.3.2, in the last two decades due to emission controls and technological advances that have led to improved air quality in most areas of Texas.

3.2. Weekly Variation in NO₂

Pollutants of anthropogenic origin are expected to exhibit weekly variation as the level of emissions resulting from the level of activity (e.g., fuel combustions) could vary during the week. In most western countries, industrial activity and traffic are reduced during the weekend, leading to lower levels of emitted pollutants (Beirle et al., 2003; Cervený & Coakley, 2002; Cleveland et al., 1974). These studies have also reported that the day of minimum NO_x emissions is generally expected for countries or metropolitan areas with some religious or cultural

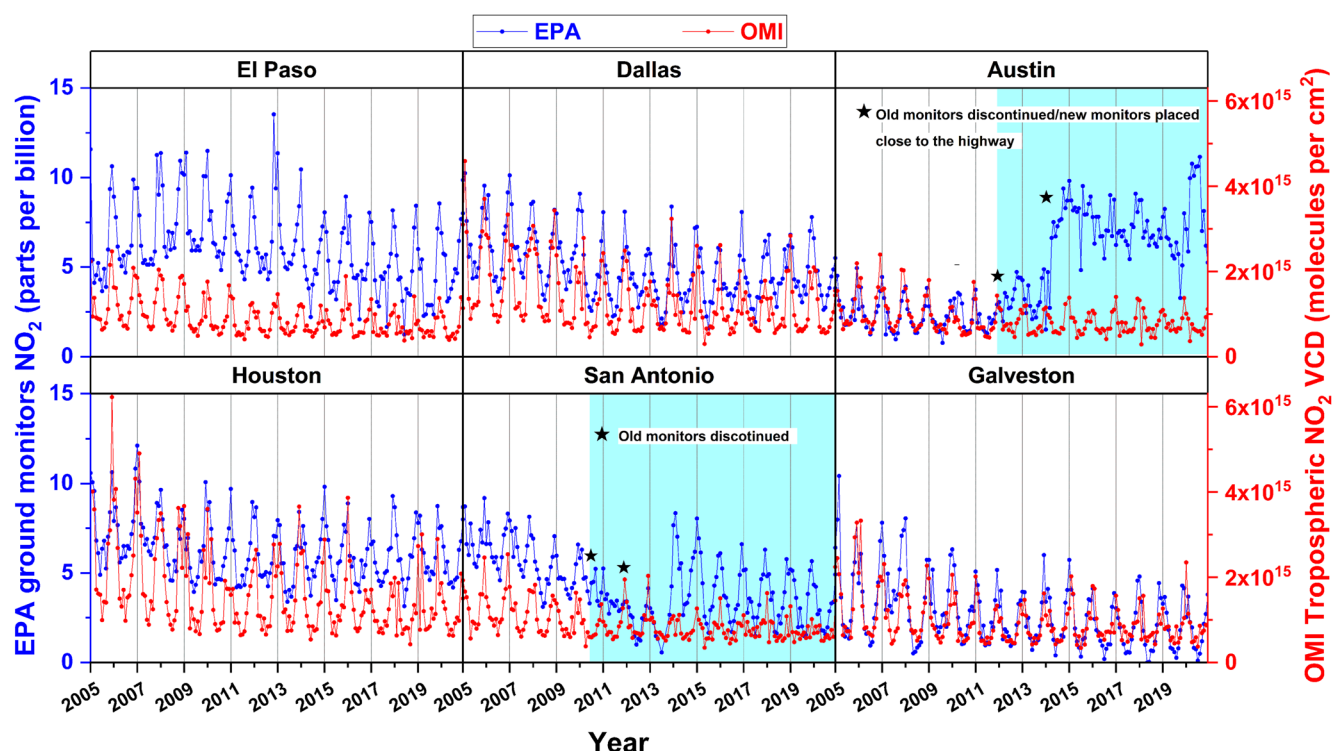


Figure 3. Time series (2005–2020) of area-averaged monthly mean values of early afternoon (1–2 PM local time) NO_2 mixing ratio (blue) from EPA monitors compared with OMI tropospheric NO_2 VCD (red) over the six cities in Texas. The shaded regions denote the record after replacing one or more monitors with new ones. The star symbols represent the instances when those discontinuities occurred.

activities on either Sunday (e.g., western countries) or Friday (e.g., Islamic cities). An analysis of the weekly variation may be helpful to characterize, discriminate, and assess various NO_x sources.

We conduct an analysis of weekly variation in NO_2 data, both in situ and remote sensing, for the cities in Texas. We explore how the weekly pattern varies over the day, how it changes in different seasons, and if it altered during the past 16 years when NO_2 declined considerably over the US. Our analysis suggests that the weekly features are generally similar for polluted metropolitan areas but could differ for areas with reduced emission sources. We show an example of a weekly variation of NO_2 pollution for Houston as a typical polluted US city and Galveston as a background area.

Figure 4 show weekly pattern in surface NO_2 mixing ratios and OMI tropospheric NO_2 VCD observed during 2005–2020 at an AQS site in Houston and Galveston. The average number of observations available for each day for OMI and surface monitors ranged, respectively, 22–41 and 45–52 annually and 5–9 and 10–13 seasonally. In Figure 4a, we show an average weekly variation in 24-hr average surface NO_2 mixing ratios compared with that at 1–2 PM, which corresponds to OMI measurement time. While the 24-hr average is higher than early afternoon values by 66% in Houston and 22% in Galveston, their weekly patterns remain consistent with a Sunday minimum. In general, Monday starts with relatively clean air. In contrast, for the other working days, the measured NO_2 might be influenced by the previous day's pollution, as the lifetime of NO_x in the troposphere is several hours to days in summer and winter, respectively. Consequently, NO_2 pollution appears to peak someday in the middle of the week. The Saturday NO_2 values decrease as compared to working days but are generally higher than that on Sundays. Over Houston, a clear Sunday minimum is evident in both in situ NO_2 mixing ratios and OMI tropospheric NO_2 VCDs (Figure 4d), with lower values on Sunday as compared to working days by 35% on the surface and 26% in OMI observations. In contrast, a much weaker weekly pattern can be observed at relatively clean Galveston Island on the Texas Gulf Coast, about 80 km southeast of Houston. Compared to working days, NO_2 levels in Galveston on Sunday are ~9% lower for both early afternoon and 24-hr average.

Figures 4b and 4e show seasonal variation in the average NO_2 weekly pattern at 1–2 PM as observed by surface monitors and OMI. While the weekly patterns are broadly consistent in all seasons, there is considerable seasonal

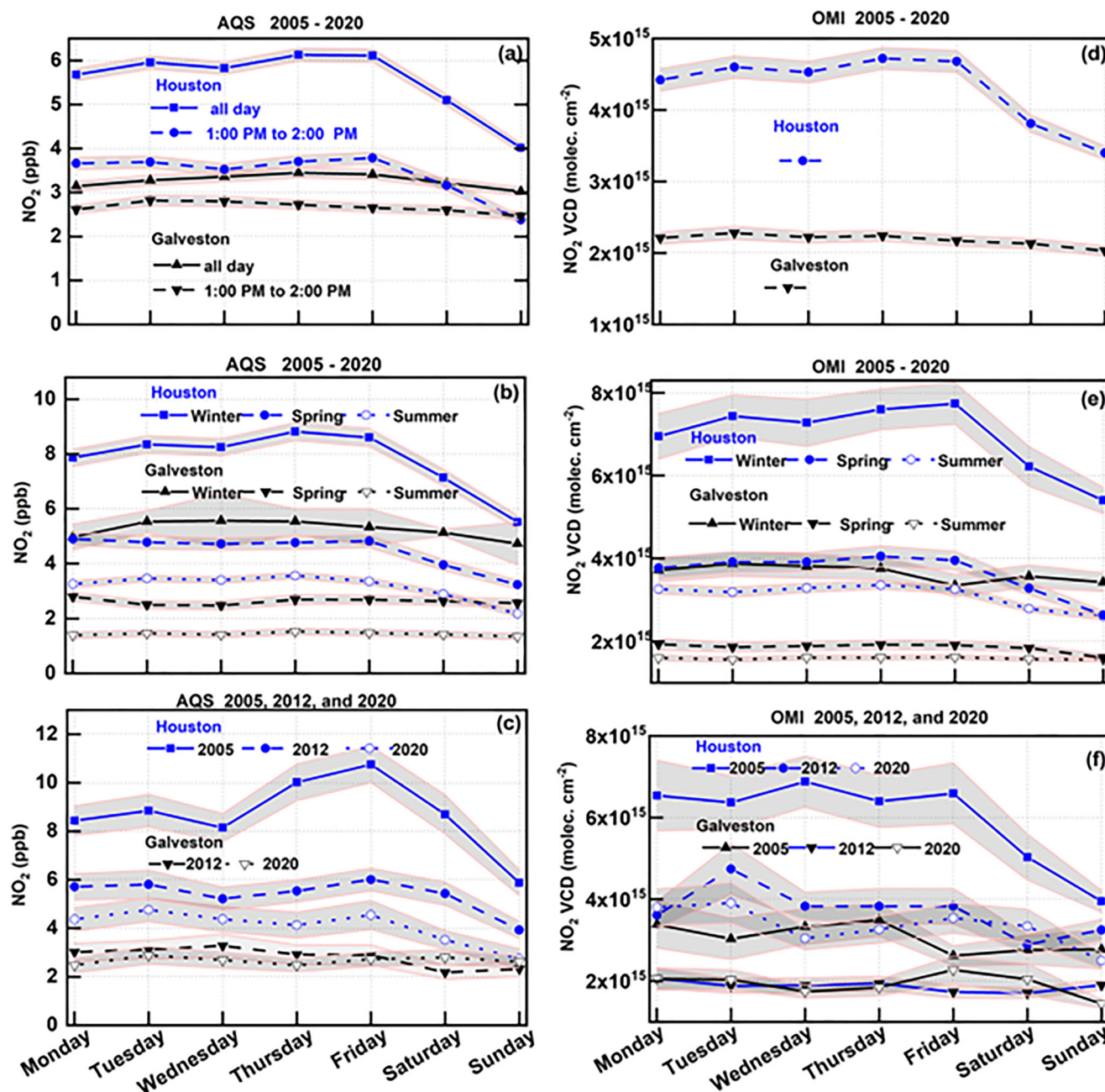


Figure 4. Mean weekly variation of NO_2 derived from the surface monitor (a–c) and OMI (d–f) data for a site in Houston (blue) and Galveston (black). (a) Weekly variation in NO_2 mixing ratios at 1–2 PM vs. 24-hr average. (b, e) Seasonal variation of weekly pattern observed in surface NO_2 mixing ratios (b) and OMI tropospheric NO_2 VCD (e) for winter, spring, and summer. (c, f) Yearly variation of weekly pattern observed in surface NO_2 mixing ratios (c) and OMI tropospheric NO_2 VCD (f) for 2005, 2012, and 2020. The shaded regions around the mean represent the standard errors of the mean.

variation due to changes in NO_x lifetime, mixing layer depth, and NO_x emissions, with maximum concentrations in winter (December–February) and minimum in summer (June–August) in both locations. The average winter to summer ratios in OMI and surface measurements are 1.2 and 1.5 for Houston and 1.3 and 2.7 for Galveston. Higher ratios for surface relative to column measurements could be due to the influence of fresh, local emissions over Houston, and several other reasons including but not limited to issues pertaining to NO_x lifetime, interferences in surface measurements, and enhanced error in satellite retrievals over the remote Galveston site. On Saturday, both surface and OMI observations show a 15%–18% NO_2 reduction. These results are consistent with those derived from Tropospheric Monitoring Instrument (TROPOMI) NO_2 observations over major US cities,

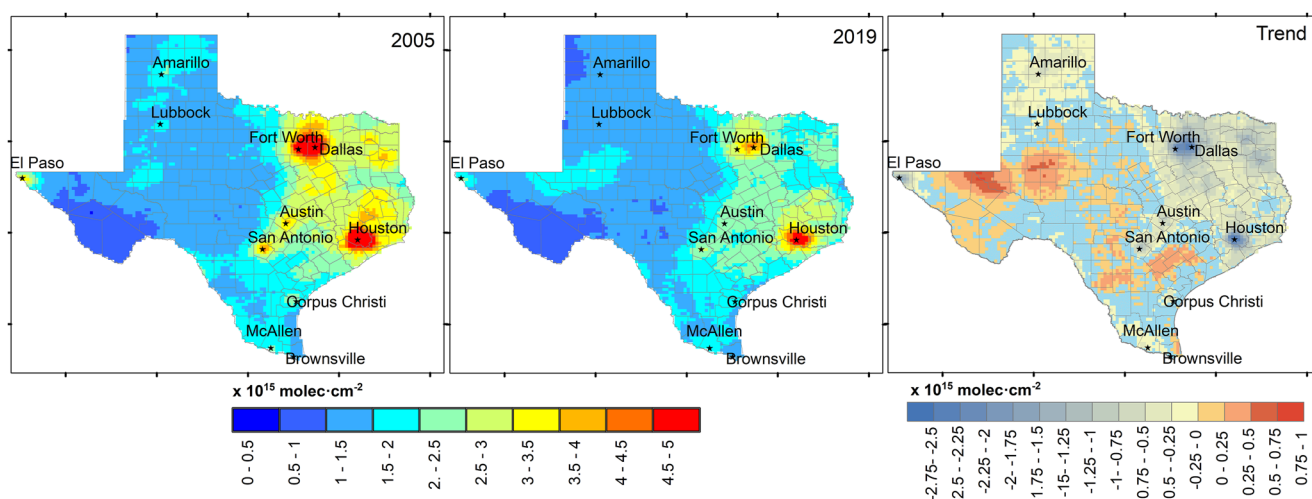


Figure 5. Annual average OMI tropospheric NO₂ VCDs over Texas at 0.1° latitude × 0.1° longitude spatial resolution for 2005 (left) and 2019 (middle). The right map shows total trend in tropospheric NO₂ columns during 2005–2019. Areas of no significant trend are indicated in the light blue color. Locations of major cities are indicated.

suggesting a reduction of 16% and 24% on Saturdays and Sundays, respectively (Goldberg, Anenberg, Kerr, et al., 2021). The magnitude of reduction differs for Sundays, with surface and OMI measurements suggesting 33%–36% and 20%–33% reductions relative to their weekday averages. Over Galveston, the weekly cycle is much weaker, with a <5% reduction on Saturday and 3%–15% on Sundays.

Figures 4c and 4f show the mean weekly cycle for 2005, 2012, and 2020. We selected these years because of overall trend patterns in the US with significant reductions from 2005 to 2010–2012, minor changes afterward, and considerable decline in 2020 due to COVID-19 restrictions as discussed in Section 3.4. The surface monitor did not exist in Galveston in 2005, but its continuous operation between 2012 and 2020 allows us to compare the weekly pattern for these years in relation to the weekly variation observed in OMI NO₂. Although we observe significant changes in NO₂ levels during 2005–2020, as discussed further in Section 3.3, the weekly patterns remain consistent with a Sunday minimum and partial reduction on Saturdays. The weekly cycle appears noisier, possibly as a result of a reduced sample size in the annual analysis, specifically for the years 2012 and 2020 when OMI lost half of the global coverage due to row anomaly (Dobber et al., 2008).

3.3. Long-Term NO₂ Trend

As evident from Figure 1, the EPA AQS network of surface monitors in Texas has sparse and uneven distribution, with the majority located in a few big cities. The network lacks observations for large regions of Texas, some of which have experienced rapid NO_x emission changes. Discontinuity of NO₂ record at a given site in the EPA network (discussed in Section 3.1) makes the assessment of NO₂ trend using surface data challenging. We take advantage of OMI's spatial coverage and stable data record to quantify NO₂ trends throughout Texas.

3.3.1. Texas-Wide Changes

Figure 5 presents the mean tropospheric NO₂ VCD for 2005 and 2019 derived from cloud-free OMI observations (effective cloud fraction <30%). We observe considerable spatial variation in tropospheric NO₂ with apparent enhancement over major cities (e.g., Dallas, Houston), industrial areas, and other source regions (e.g., oil and natural gas extraction). These maps reveal significant changes in NO₂ pollution between 2005 and 2019, with a substantial reduction in eastern Texas, particularly over cities, and some enhancement over oil and natural gas extraction regions in the western part of Texas.

Using the multivariate linear regression analysis described in Section 2.3, we calculate the linear trend in tropospheric NO₂ VCDs. The right map in Figure 5 shows total changes (calculated from $L \cdot t$ in Equation 1) during the years 2005–2019. Three distinct areas are evident. The East Texas regions and most cities exhibit a negative trend, the oil and gas producing areas of West Texas have a positive trend, and the central part lacks any

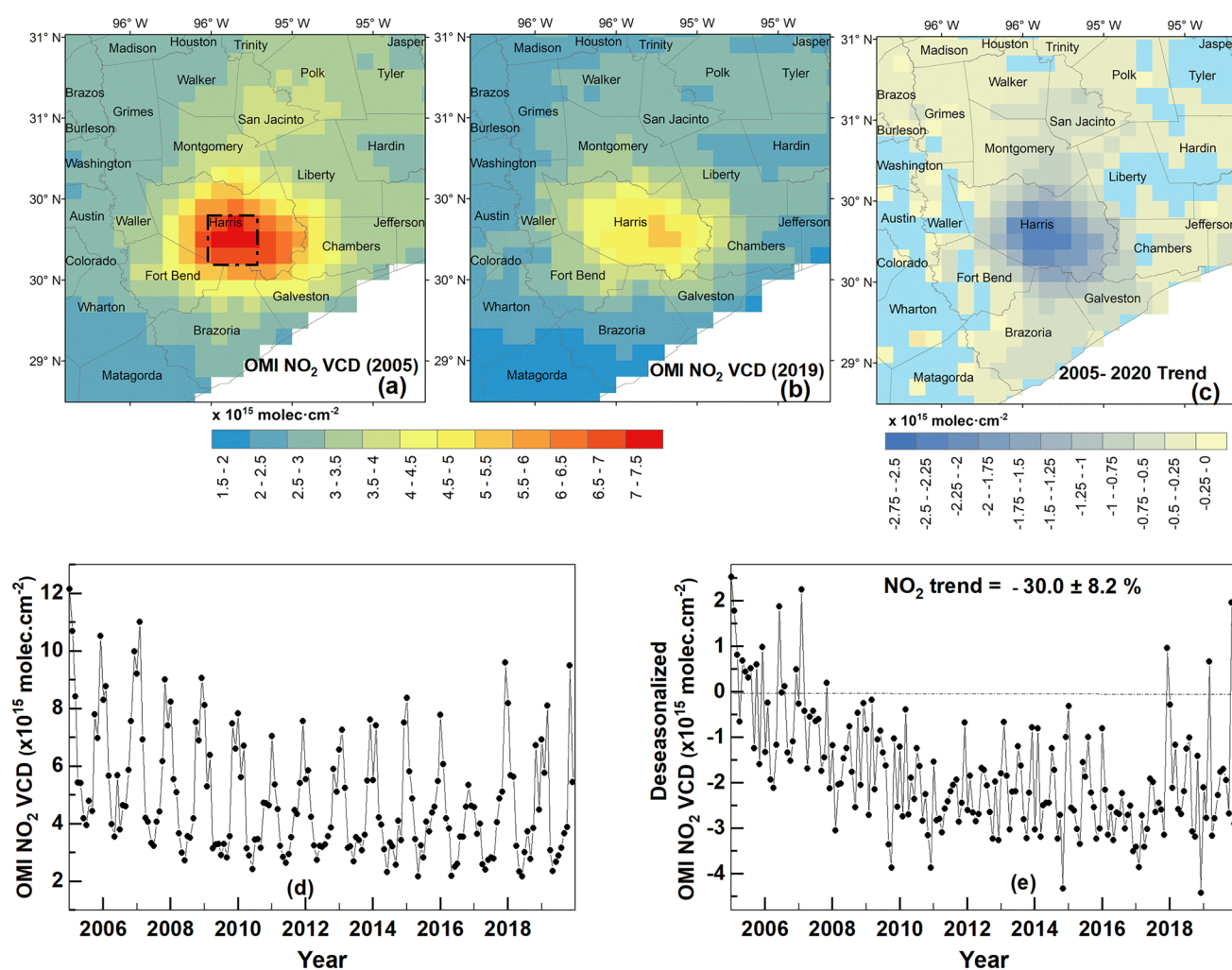


Figure 6. Changes in OMI NO₂ tropospheric VCD from 2005 to 2019 over Houston, Texas. The top row shows the annual average for (a) 2005, (b) 2019, and (c) total changes between 2005 and 2019 derived from the linear trend discussed in Section 2.3. The light blue color in (c) represents the area with a statistically insignificant trend at 95% confidence. The spatial resolution of the data is 0.1° latitude × 0.1° longitude. The bottom row shows the time series of (d) monthly average OMI tropospheric NO₂ VCD data and (e) their de-seasonalized values averaged over a box of size 0.3° × 0.3° over Houston as indicated by a square box in the 2005 map (a). The dotted line in figure (e) represents the 2005 baseline. The total trend and its uncertainty over the enclosed area in Houston are indicated.

clear trend. The largest changes have occurred where NO₂ levels are high. A sizable positive trend visible over Permian and other basins will be discussed further in Section 3.3.3. Large and statistically significant decreasing trends are observed in major urban areas, specifically in and around Dallas and Houston and a few spots in Austin and San Antonio. Texas has been part of the Clean Air Interstate Rule (CAIR) and Cross-State Air Pollution Rule (CSAPR) issued by EPA that implemented a “cap and trade” system to reduce NO_x and other pollutants. NO_x emissions also decreased in 2008 due to the global economic downturn (Tong et al., 2016) and 2020 due to COVID-19 (Cooper et al., 2022; Huang et al., 2021; Keller et al., 2021) restrictions, both of which were captured in OMI NO₂ levels. Moreover, there have been significant reductions in vehicular emissions over the past few decades due to advances in engine and emission control technologies to meet increasingly stringent regulations (Bishop & Stedman, 2008).

3.3.2. Changes in Major Cities

Figure 6 displays the spatial (0.1° latitude × 0.1° longitude) and temporal (monthly and annual averages) variation of OMI tropospheric NO₂ VCDs for Houston, TX. Figures 6a and 6b show the spatial distribution of annual average OMI NO₂ levels in 2005 and 2019. While the data for both years show clear enhancement over central Houston, notably in Harris County, we observe the area-wide, albeit non-uniform, reductions from 2005 to 2019.

Figure 6c shows the spatial pattern in the total decrease in OMI tropospheric NO₂ levels, showing the largest absolute reductions over Harris County and its neighborhood. The changes are substantial and statistically significant over most of the 5° latitude × 5° longitude domain centered around Houston. Figure 6d shows monthly tropospheric NO₂ VCDs over an area of size 0.3° latitude × 0.3° longitude in central Houston. As evident from the figure, a large portion of tropospheric NO₂ variations arises from seasonal changes driven mostly by NO_x chemistry with wintertime maximum. Isolation of long-term causes and transient, short-term fluctuations emanating from weather and other events, as presented in Figure 6e, allows us to infer total change and its uncertainty in OMI NO₂ levels over Houston.

We conducted a similar analysis for 42 large cities of Texas having over 100,000 population in 2020. Figure 7 presents the total NO₂ trends during 2005–2019. Of these 42 cities, percent reductions are in the range of 30%–36% in 9 cities, 20%–30% in 15 cities, 10%–20% in 10 cities, and 0%–10% in 3 cities. The largest percent decreases occurred in highly populated cities (e.g., Dallas with $33.3 \pm 6.9\%$ decrease, Houston with $30.1 \pm 8.2\%$ decrease) and their surrounding regions (e.g., Lewisville with $32.7 \pm 6.8\%$ decrease) with high emission levels. These results, while based on improved and longer OMI NO₂ records, are broadly consistent with the work of Lamsal et al. (2015) and Duncan et al. (2016) for the cities in Texas. Similar reductions of ~35% have been reported in US cities by Goldberg, Anenberg, Lu, et al. (2021). Three cities located near the shale region in West Texas showed increasing trends in NO₂ level. Those include Midland ($25.7 \pm 8.5\%$), Odessa ($11.2 \pm 7.8\%$), and San Angelo ($7.6 \pm 8.0\%$). Observed changes in OMI NO₂ levels in these and other cities close to the Shale regions result from a complex interplay of fast-growing industrial areas, enhanced activities, and existing regulations intended for limiting NO_x emissions, as discussed earlier.

3.3.3. Changes in Shale Regions

In this section, we examine trends of OMI NO₂ VCD and relate them to oil and Natural gas production during 2007–2019 for Texas's three major shale zones: Permian, Eagle Ford, and Haynesville.

Figure 8a shows the spatial distribution of the OMI VCD NO₂ trend (in percent) over Texas's three shale plays. A substantial (up to 85%) increase in NO₂ is observed over Reeves, Martin, Howard, and other counties in Permian Basin, resulting from continuous, rapid rise in gas and oil production over the past several years. Similarly, most of the counties in Eagle Ford exhibited an increase in NO₂ levels, however, to a lesser extent than the Permian Basin. In contrast, we observe a decline in NO₂ levels nearly everywhere in Haynesville except over Nacogdoches County.

In Figures 8b–8d, we examine the temporal variation of de-seasonalized OMI tropospheric NO₂ VCDs over shale regions and relate them to the changes in their respective gas and oil production capacities. Since seasonal patterns dominate a large part of NO₂ variation, we isolate the seasonal component from OMI NO₂ data and consider the de-seasonalized OMI NO₂ values. Over the shale plays, there is considerable spatial variation in NO₂ trends ranging from non-significant to high positive/negative trends. To relate OMI NO₂ trends with oil and gas productions, we only consider the geographic areas that have significant and largest trends (higher than 87th percentile from the distribution) for each of the three shale regions; this helps maximize NO₂ signals from oil and natural gas operations and reduces the noise contribution from surrounding areas. On the right y-axes of Figures 8b–8d, we present the oil and gas production amounts, which tend to increase or decrease in concert from 2007 to 2019. These data on production statistics and drilling rig counts available after 2007 only are taken from the U.S. Energy Information Administration's database (US EIA, 2021). The de-seasonalized OMI NO₂ VCD levels in the three shale regions have declined or remained steady from 2007 to 2015, mainly attributed to a low-production phase of oil and natural gas production. NO₂ pollution has risen significantly since 2016 in the Permian Basin and from 2010 to 2015 in the Eagle Ford shale plays in line with the regional oil and gas production. The monthly average OMI NO₂ VCDs are found to significantly correlate with gross oil ($r = 0.65$) and gas ($r = 0.63$) productions in Permian Basin and to a lesser degree in Eagle Ford ($r = 0.38$). The relationship strengthened considerably in annually-averaged values with a correlation coefficient close to 0.88 and is consistent with prior work by Dix et al. (2020). Diesel engine operation and raw gas combustion in flares contribute to the increase in ambient NO₂ (Gorchov Negron et al., 2018). In contrast, Haynesville gas production shows a roughly linear decline, falling by more than a factor of two since the year 2007. The correlation between the de-seasonalized OMI NO₂ VCD and oil and gas production is relatively poor ($r = 0.17$), although the correlation improves considerably ($r = 0.62$) with annually-averaged values. These results are consistent with prior studies by Majid et al. (2017), who used an earlier version of the OMI NO₂ product (Bucsela et al., 2013; Lamsal et al., 2014) and a shorter data record. The

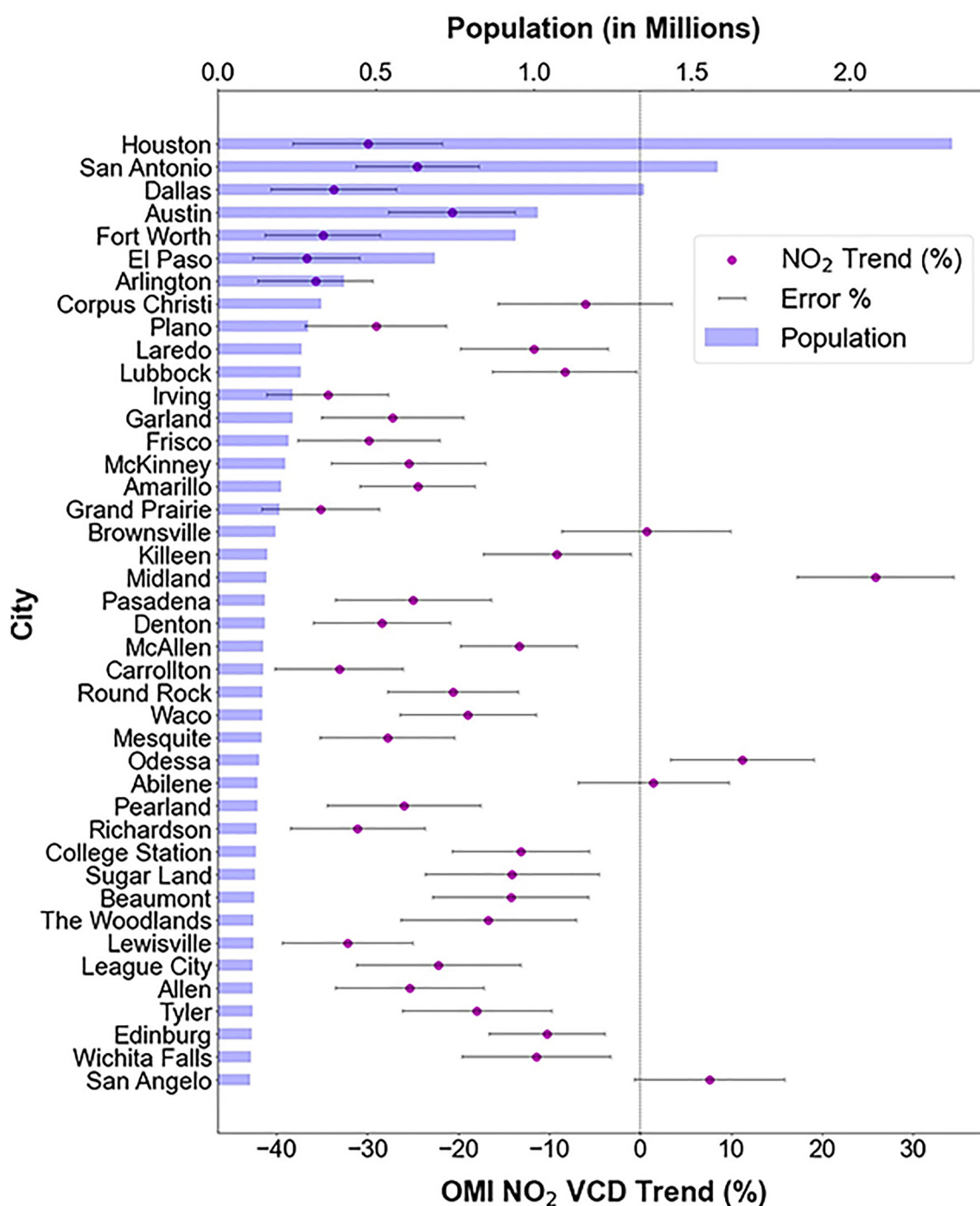


Figure 7. OMI NO₂ trend from 2005 to 2019 along with the percentage error (at 95% confidence levels) for the 42 largest cities in Texas with more than 100,000 population.

lower values of the correlation coefficient at Haynesville compared to the two oil-producing regions are likely due to the lack of oil production and its proximity to an urbanized area.

3.4. COVID-19-Driven NO₂ Changes

The unprecedented measures imposed by national and local governments to reduce the spread of COVID-19 had a dramatic impact on air pollution with a significant drop in pollutants' concentrations, notably in NO₂,

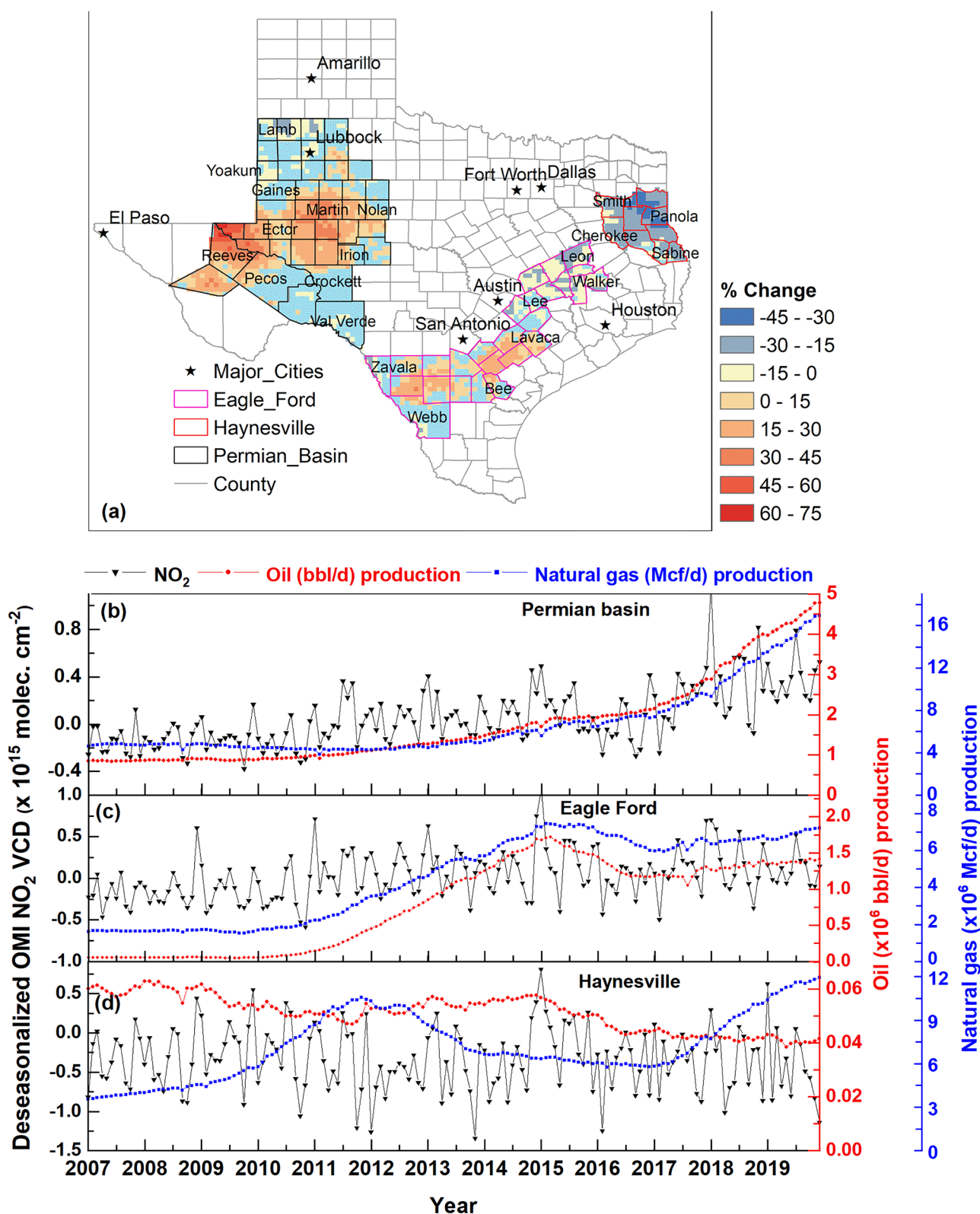


Figure 8. Changes in OMI de-seasonalized NO₂ levels over Texas's three shale oil regions. (a) Percent change in OMI NO₂ VCD data between 2007 and 2019 for the Eagle Ford, Permian, and Haynesville basins. The resolution of the data is 0.1° latitude × 0.1° longitude. The light blue color in (a) represents the area with the statistically insignificant trend at 95% confidence. The line plots show the time series of monthly de-seasonalized OMI tropospheric NO₂ VCD (left y-axis, black line) and monthly oil (right y-axis, red) and natural gas (right y-axis, blue) production over (b) Permian, (c) Eagle Ford, and (d) Haynesville basins.

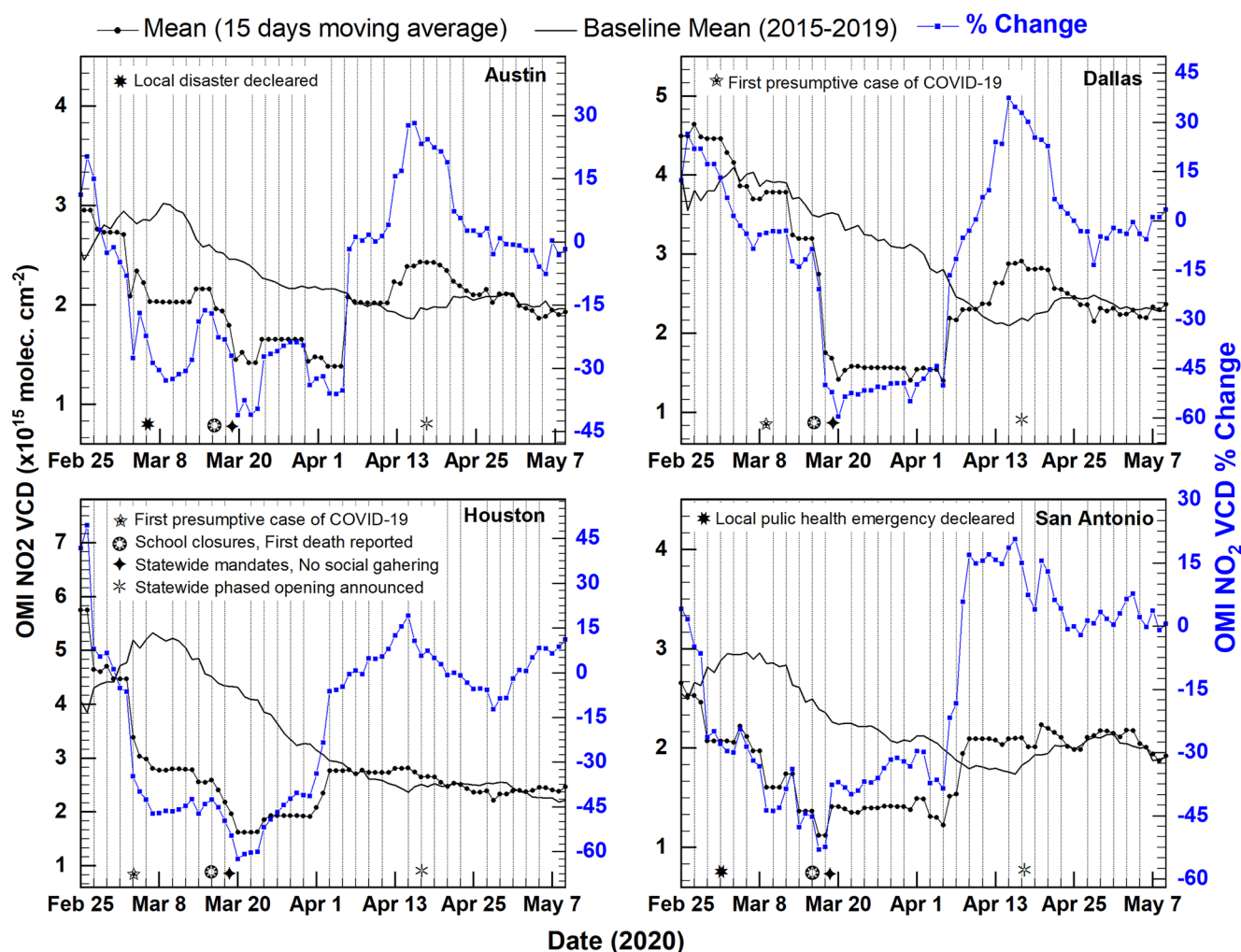


Figure 9. Time series of OMI NO₂ VCD with a 15-day (within ± 7 days) moving average for Austin (top left), Dallas (top right), Houston (bottom left), and San Antonio (bottom right) from Feb 25 to May 10. The dotted black line shows the mean NO₂ (for 2020), the solid black line indicates the 5-year (2015–2019) baseline mean, and the blue line represents the % change in NO₂ levels, which is the difference between the 2020 mean, and the baseline mean values. Major COVID-related events are noted.

due to reduced transport, industrial, and other economic activities involving fossil fuel combustion (Bauwens et al., 2020; Forster et al., 2020; Huang et al., 2021; Liu et al., 2020). In Texas, starting 1 March 2020, there were a series of provisions and restrictions at local, state, and federal levels to contain the spread of the virus and protect public health during the pandemic. The first public health emergency was declared in San Antonio on March 1st; that Austin followed on March 6 through a local disaster declaration (Limón, 2020; Newsroom, 2021). On March 11, WHO declared COVID-19 as a pandemic when universities and colleges in Texas switched to online classes (Agency, 2022). Coinciding with the declaration of COVID-19 as a national emergency, a statewide public health disaster was declared on March 13. The Centers for Disease Control and Prevention put limits on the number of public gatherings on March 15 for the next 8 weeks. After the first covid-related Texan death on March 15, Dallas and Houston closed bars and clubs and put severe limits on restaurants the following day. Days later, on March 19, similar restrictions were issued at the state level. The country's southern border was closed on March 20. After Dallas County ordered residents to shelter in place on March 22, other larger counties issued stay-at-home orders on March 23. Between March 26 and 31, the state government issued multiple travel restrictions and school closures. Figure 9 shows how each of these events relates to changes in OMI NO₂ levels in four major cities in Texas. Shown are 15-day running averages between February 25 and May 10 in 2020 compared with corresponding values derived from the previous five years (2015–2019), referred to as the baseline. Using a baseline as a reference help reduce the effect of short-term changes arising from yearly variation in weather patterns and

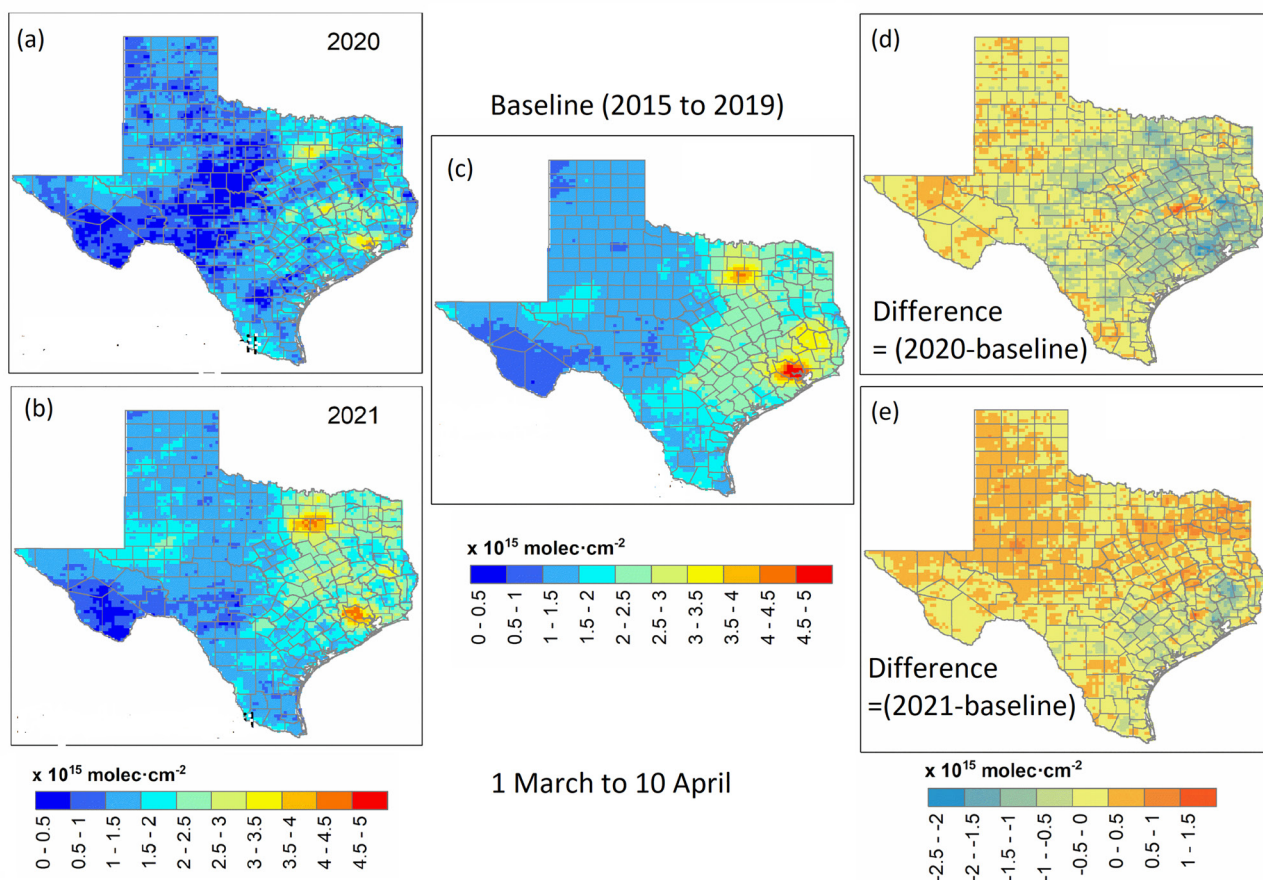


Figure 10. Average OMI tropospheric NO₂ VCDs (at 0.1° latitude x 0.1° longitude resolution) from 1 March to 10 April of (a) 2020, (b) 2021, and (c) 2015–2019 (baseline). The right panels show the difference of baseline from (d) 2020, and (e) 2021.

random noise in OMI data. The city domain covers a 1° × 1° box around the city center. Additional details on these time-series data used here can be found on NASA's Global Nitrogen Dioxide Monitoring webpage (https://so2.gsfc.nasa.gov/no2/no2_index.html). It is evident from Figure 9 that the most significant decline in OMI NO₂ occurred around 20 March 2020, reaching up to 60% in Houston and Dallas and a somewhat lower decrease in San Antonio and Austin. Temporal variations exist between cities, reflecting local scenarios and responses. Unlike in other cities in the eastern and western US, OMI NO₂ levels in all these cities appear to rebound in the first 2 weeks of April. To put these short-term reductions into context, the COVID-driven changes appear to be higher than the reductions achieved in the past 16 years through long-term sustained efforts in technology advancement and regulations.

To examine the COVID-driven changes over all of Texas, we compare the 40-day (March 1–April 10) average OMI NO₂ for 2020 and 2021 against the data averaged over the same period in 2015–2019 (baseline). Figures 10a–10c show the spatial distribution of OMI NO₂ VCDs in 2020, 2021, and baseline years. The enhanced noise in 2020 is due to a limited number of cloud-free OMI observations used in the 2020 average and nearly a factor of five more observations available for the baseline. While the three maps exhibit similarities in spatial pattern, we observe a substantial reduction in 2020, especially over urban and densely populated areas in eastern Texas and bouncing back in 2021. The difference in NO₂ levels from 2020 to 2021 to the baseline shown in the right panel of Figure 10 depicts a complex picture with a wide range of values ranging from negative to positive, suggesting a reduction reflecting non-uniform local responses to COVID in 2020 and a rebound in NO₂ levels in 2021 as well as the influence of observational noise and changing weather patterns.

4. Summary and Conclusions

We analyzed the changes in nitrogen dioxide (NO_2) pollution for the year 2005–2020 over Texas utilizing tropospheric NO_2 column data from OMI/Aura and in situ surface NO_2 measurements from the US EPA AQS and TCEQ networks. We examined the relationship between these two measurements over 38 sites in six major cities. The correlations between daily AQS and OMI observations vary from 0.2 to 0.8 depending on monitor locations with higher correlation for polluted sites. The correlation coefficients were found to increase significantly (varied from $r = 0.5$ to $r = 0.9$) for paired monthly average values. Our analysis of weekly variation of OMI and surface NO_2 observations as a whole set as well as its partitioning by seasons and years demonstrate a highly consistent weekly pattern suggesting that NO_2 levels on Saturday and Sunday relative to weekdays are respectively $\sim 15\%$ and 30% lower for the polluted area in Houston and $\sim 5\%$ and 9% lower for clean background area in Galveston. Given the difference in parameter (column by OMI vs. mixing ratio by surface monitors) and resolution (tens of square km for OMI vs. in situ for ground monitors) the observed correspondence between OMI and surface observations is remarkable and is of significance for observing surface level NO_2 pollution from space.

With statistical analysis, NO_2 trends and their uncertainties were examined over Texas, including 42 large cities with a population higher than 100,000. Most regions showed a significant decrease in NO_2 , especially for highly populated cities; all cities show negative trends except for shale oil regions. Of these 42 cities, percent reductions are 30% – 36% in 09 cities, 20% – 30% in 15 cities, 10% – 20% in 10 cities, and 0% – 10% for four cities. The highly populated cities of Houston (NO_2 reduction $30.0 \pm 8.2\%$) and Dallas (NO_2 reduction $33.34 \pm 6.9\%$) are among the cities with the largest NO_2 reductions. In contrast, we observe a significant rise in tropospheric NO_2 pollution over shale oil and natural gas development regions of the Permian (up to 80%) and Eagle Ford (up to 30%) basins during 2005–2019. The change in NO_2 levels in these regions correlated well ($r = 0.7$ – 0.9) with the oil and gas production levels.

Notable decreases in OMI NO_2 levels were observed over widespread areas in Texas in March–April 2020. Those decreases are evident from comparing NO_2 levels before, during, and after the lockdown and when contrasting the 2020 levels with those during the same period in 2015–2019 and 2021. The NO_2 levels decreased 40% and 60% in Austin and Houston, respectively, during the national and local stay-at-home orders and other restrictions. We observe near-complete rebound in NO_2 levels in 2021. The temporary decreases that lasted only for a couple of weeks were due to the stay-at-home measures against the spread of the Covid-19, which caused sharp reductions in traffic and industrial activities.

Conflict of Interest

The authors declare no conflicts of interest relevant to this study.

Data Availability Statement

OMI data can be freely downloaded from the NASA Aura Validation Data Center website (<https://avdc.gsfc.nasa.gov/pub/data/satellite/Aura/OMI/V03/L3/>), Air Quality System Data can be freely downloaded from, https://aqs.epa.gov/aqsweb/airdata/download_files.html; similarly, TCEQ data from, <https://www17.tceq.texas.gov/tamis/index.cfm>, and Oil and Natural gas production data can be freely downloaded from <https://www.eia.gov/state/?sid=TX>.

References

- Agency, T. E. (2022). Coronavirus (COVID-19) support and guidance. Retrieved from <https://tea.texas.gov/texas-schools/health-safety-discipline/covid/coronavirus-covid-19-support-and-guidance>
- American Lung Association. (2022). Most polluted cities. Retrieved from <https://www.lung.org/research/sota/city-rankings/most-polluted-cities>
- Anderson, D. C., Loughner, C. P., Diskin, G., Weinheimer, A., Canty, T. P., Salawitch, R. J., et al. (2014). Measured and modeled CO and NOy in DISCOVER-AQ: An evaluation of emissions and chemistry over the eastern US. *Atmospheric Environment*, 96, 78–87. <https://doi.org/10.1016/j.atmosenv.2014.07.004>
- Banta, R. M., Senff, C. J., Nielsen-Gammon, J., Darby, L. S., Ryerson, T. B., Alvarez, R. J., et al. (2005). A bad air day in Houston. *Bulletin of the American Meteorological Society*, 86(5), 657–670. <https://doi.org/10.1175/BAMS-86-5-657>
- Bauwens, M., Compernelle, S., Stavrakou, T., Müller, J.-F., Gent, J., Eskes, H., et al. (2020). Impact of coronavirus outbreak on NO_2 pollution assessed using TROPOMI and OMI observations. *Geophysical Research Letters*, 47(11), e2020GL087978. <https://doi.org/10.1029/2020GL087978>

Acknowledgments

We would like to thank Dr. Christopher Wild and San Jacinto College, Texas, for facilitating this research and collaboration with various agencies and Universities. We acknowledge the free publicly available OMI data from the NASA Aura Validation Data Center website (<https://avdc.gsfc.nasa.gov/pub/data/satellite/Aura/OMI/V03/L3/>), Air Quality System Data Mart [internet database] via https://aqs.epa.gov/aqsweb/airdata/download_files.html.%20accessed%2020%20March%2021, TCEQ data [internet database] via <https://www17.tceq.texas.gov/tamis/index.cfm>, accessed 10 October 2022, and Oil and Natural gas production data [internet database] via <https://www.eia.gov/state/?sid=TX>, accessed 20 March 2021. Finally, we would like to thank Dr. Gunnar Schade, Dr. Joshua Laughner, and two anonymous reviewers for reviewing and providing helpful comments that helped improve this manuscript.

- Bechle, M. J., Millet, D. B., & Marshall, J. D. (2013). Remote sensing of exposure to NO₂: Satellite versus ground-based measurement in a large urban area. *Atmospheric Environment*, 69, 345–353. <https://doi.org/10.1016/j.atmosenv.2012.11.046>
- Beirle, S., Platt, U., Wenig, M., & Wagner, T. (2003). Weekly cycle of NO₂ by GOME measurements: A signature of anthropogenic sources. *Atmospheric Chemistry and Physics*, 3(6), 2225–2232. <https://doi.org/10.5194/acp-3-2225-2003>
- Berkowitz, C. M., Spicer, C. W., & Doskey, P. V. (2005). Hydrocarbon observations and ozone production rates in Western Houston during the Texas 2000 air quality study. *Atmospheric Environment*, 39(19), 3383–3396. <https://doi.org/10.1016/j.atmosenv.2004.12.007>
- Bishop, G. A., & Stedman, D. H. (2008). A decade of on-road emissions measurements. *Environmental Science & Technology*, 42(5), 1651–1656. <https://doi.org/10.1021/es702413b>
- Boersma, K. F., Eskes, H. J., Veeffkind, J. P., Brinksma, E. J., Levelt, P. F., Stammes, P., et al. (2007). Near-real time retrieval of tropospheric NO₂ from OMI. *Atmospheric Chemistry and Physics*, 16.
- Boersma, K. F., Jacob, D. J., Bucsela, E. J., Perring, A. E., Dirksen, R., vanderA, R. J., et al. (2008). Validation of OMI tropospheric NO₂ observations during INTEX-B and application to constrain NO_x emissions over the eastern United States and Mexico. *Atmospheric Environment*, 42(19), 4480–4497. <https://doi.org/10.1016/j.atmosenv.2008.02.004>
- Bradshaw, J., Davis, D., Grodzinsky, G., Smyth, S., Newell, R., Sandholm, S., & Liu, S. (2000). Observed distributions of nitrogen oxides in the remote free troposphere from the Nasa Global Tropospheric Experiment Programs. *Reviews of Geophysics*, 38(1), 61–116. <https://doi.org/10.1029/1999RG900015>
- Bucsela, E. J., Krotkov, N. A., Celarier, E. A., Lamsal, L. N., Swartz, W. H., Bhartia, P. K., et al. (2013). A new stratospheric and tropospheric NO₂ retrieval algorithm for nadir-viewing satellite instruments: Applications to OMI. *Atmospheric Measurement Techniques*, 6(10), 2607–2626. <https://doi.org/10.5194/amt-6-2607-2013>
- Bunch, A. G., Perry, C. S., Abraham, L., Wikoff, D. S., Tachovsky, J. A., Hixon, J. G., et al. (2014). Evaluation of impact of shale gas operations in the Barnett Shale region on volatile organic compounds in air and potential human health risks. *Science of the Total Environment*, 468–469, 832–842. <https://doi.org/10.1016/j.scitotenv.2013.08.080>
- Bureau, U. C. (2017). Births and migration push population to nearly 28 million. Retrieved from <https://www.census.gov/library/stories/2017/08/texas-population-trends.html>
- Bureau, U. C. (2020). Texas added almost 4 million people in last decade. Retrieved from <https://www.census.gov/library/stories/state-by-state/texas-population-change-between-census-decade.html>
- Buzcu-Guven, B., & Fraser, M. (2008). Comparison of VOC emissions inventory data with source apportionment results for Houston, TX. *Atmospheric Environment*, 42(20), 5032–5043. <https://doi.org/10.1016/j.atmosenv.2008.02.025>
- Byun, D. W., Kim, S., Czader, B., Nowak, D., Stetson, S., & Estes, M. (2005). Estimation of biogenic emissions with satellite-derived land use and land cover data for air quality modeling of Houston-Galveston ozone nonattainment area. *Journal of Environmental Management*, 75(4), 285–301. <https://doi.org/10.1016/j.jenvman.2004.10.009>
- Caicedo, V., Rappenglueck, B., Cuchiara, G., Flynn, J., Ferrare, R., Scarino, A. J., et al. (2019). Bay Breeze and Sea Breeze circulation impacts on the planetary boundary layer and air quality from an observed and Modeled DISCOVER-AQ Texas case study. *Journal of Geophysical Research: Atmospheres*, 124(13), 7359–7378. <https://doi.org/10.1029/2019JD030523>
- Cerveny, R., & Coakley, K. J. (2002). A weekly cycle in atmospheric carbon dioxide. *Geophysical Research Letters*, 29(2), 151–154. <https://doi.org/10.1029/2001GL013952>
- Chen, F., Miao, S., Tewari, M., Bao, J.-W., & Kusaka, H. (2011). A numerical study of interactions between surface forcing and sea breeze circulations and their effects on stagnation in the greater Houston area. *Journal of Geophysical Research*, 116(D12), D12105. <https://doi.org/10.1029/2010JD015533>
- Cleveland, W. S., Graedel, T. E., Kleiner, B., & Warner, J. L. (1974). Sunday and weekday variations in photochemical air pollutants in New Jersey and New York. *Science*, 186(4168), 1037–1038. <https://doi.org/10.1126/science.186.4168.1037>
- Cohen, A. J., Brauer, M., Burnett, R., Anderson, H. R., Frostad, J., Estep, K., et al. (2017). Estimates and 25-year trends of the global burden of disease attributable to ambient air pollution: An analysis of data from the Global Burden of Diseases Study 2015. *The Lancet*, 389(10082), 1907–1918. [https://doi.org/10.1016/S0140-6736\(17\)30505-6](https://doi.org/10.1016/S0140-6736(17)30505-6)
- Cooper, M. J., Martin, R. V., Hammer, M. S., Levelt, P. F., Veeffkind, P., Lamsal, L. N., et al. (2022). Global fine-scale changes in ambient NO₂ during COVID-19 lockdowns. *Nature*, 601(7893), 380–387. <https://doi.org/10.1038/s41586-021-04229-0>
- Crutzen, P. J. (1979). The role of NO and NO₂ in the chemistry of the troposphere and stratosphere. *Annual Review of Earth and Planetary Sciences*, 7(1), 443–472. <https://doi.org/10.1146/annurev.ear.07.050179.002303>
- Cushing, L. J., Chau, K., Franklin, M., & Johnston, J. E. (2021). Up in smoke: Characterizing the population exposed to flaring from unconventional oil and gas development in the contiguous US. *Environmental Research Letters*, 16(3), 034032. <https://doi.org/10.1088/1748-9326/abd3d4>
- Daum, P. H., Kleinman, L. I., Springston, S. R., Nunnermacker, L. J., Lee, Y.-N., Weinstein-Lloyd, J., et al. (2003). A comparative study of O₃ formation in the Houston urban and industrial plumes during the 2000 Texas Air Quality Study. *Journal of Geophysical Research*, 108(D23), 4715. <https://doi.org/10.1029/2003JD003552>
- Demerjian, K. L. (2000). A review of national monitoring networks in North America. *Atmospheric Environment*, 34(12), 1861–1884. [https://doi.org/10.1016/S1352-2310\(99\)00452-5](https://doi.org/10.1016/S1352-2310(99)00452-5)
- Demetillo, M. A. G., Navarro, A., Knowles, K. K., Fields, K. P., Geddes, J. A., Nowlan, C. R., et al. (2020). Observing nitrogen dioxide air pollution inequality using high-spatial-resolution remote sensing measurements in Houston, Texas. *Environmental Science & Technology*, 54(16), 9882–9895. <https://doi.org/10.1021/acs.est.0c01864>
- Dix, B., de Bruin, J., Roosenbrand, E., Vlemmix, T., Francoeur, C., Gorchov-Negron, A., et al. (2020). Nitrogen oxide emissions from U.S. oil and gas production: Recent trends and source attribution. *Geophysical Research Letters*, 47(1), e2019GL085866. <https://doi.org/10.1029/2019GL085866>
- Dobber, M., Kleipool, Q., Dirksen, R., Levelt, P., Jaross, G., Taylor, S., et al. (2008). Validation of ozone monitoring instrument level 1b data products. *Journal of Geophysical Research*, 113(D15), D15S06. <https://doi.org/10.1029/2007JD008665>
- Duncan, B. N., Lamsal, L. N., Thompson, A. M., Yoshida, Y., Lu, Z., Streets, D. G., et al. (2016). A space-based, high-resolution view of notable changes in urban NO₂ pollution around the world (2005–2014). *Journal of Geophysical Research: Atmospheres*, 121(2), 976–996. <https://doi.org/10.1002/2015JD024121>
- Fan, J., Zhang, Y., Li, Z., Hu, J., & Rosenfeld, D. (2020). Urbanization-induced land and aerosol impacts on sea-breeze circulation and convective precipitation. *Atmospheric Chemistry and Physics*, 20(22), 14163–14182. <https://doi.org/10.5194/acp-20-14163-2020>
- Farmer, S. A., Nelin, T. D., Falvo, M. J., & Wold, L. E. (2014). Ambient and household air pollution: Complex triggers of disease. *American Journal of Physiology - Heart and Circulatory Physiology*, 307(4), H467–H476. <https://doi.org/10.1152/ajpheart.00235.2014>

- Field, R. A., Soltis, J., & Murphy, S. (2014). Air quality concerns of unconventional oil and natural gas production. *Environmental Sciences: Processes & Impacts*, 16(5), 954–969. <https://doi.org/10.1039/C4EM00081A>
- Forster, P. M., Forster, H. I., Evans, M. J., Gidden, M. J., Jones, C. D., Keller, C. A., et al. (2020). Current and future global climate impacts resulting from COVID-19. *Nature Climate Change*, 10(10), 913–919. <https://doi.org/10.1038/s41558-020-0883-0>
- Goldberg, D. L., Anenberg, S. C., Kerr, G. H., Moheggh, A., Lu, Z., & Streets, D. G. (2021). TROPOMI NO₂ in the United States: A detailed look at the annual averages, weekly cycles, effects of temperature, and correlation with surface NO₂ concentrations. *Earth's Future*, 9(4), e2020EF001665. <https://doi.org/10.1029/2020EF001665>
- Goldberg, D. L., Anenberg, S. C., Lu, Z., Streets, D. G., Lamsal, L. N., E McDuffie, E., & Smith, S. J. (2021b). Urban NO_x emissions around the world declined faster than anticipated between 2005 and 2019. *Environmental Research Letters*, 16(11), 115004. <https://doi.org/10.1088/1748-9326/ac2c34>
- Gorchov Negron, A. M., McDonald, B. C., McKeen, S. A., Peischl, J., Ahmadov, R., de Gouw, J. A., et al. (2018). Development of a fuel-based oil and gas inventory of nitrogen oxides emissions. *Environmental Science & Technology*, 52(17), 10175–10185. <https://doi.org/10.1021/acs.est.8b02245>
- Huang, X., Ding, A., Gao, J., Zheng, B., Zhou, D., Qi, X., et al. (2021). Enhanced secondary pollution offset reduction of primary emissions during COVID-19 lockdown in China. *National Science Review*, 8(2), nwaa137. <https://doi.org/10.1093/nsr/nwaa137>
- Jacob, D. J., & Winner, D. A. (2009). Effect of climate change on air quality. *Atmospheric Environment*, 43(1), 51–63. <https://doi.org/10.1016/j.atmosenv.2008.09.051>
- Jensen, M., Fan, J., Collis, S., Bruning, E., Giangrande, S., Pal, S., et al. (2021). Aerosol, cloud, precipitation and climate (ACPC) initiative deep convection cloud roadmap.
- Jobson, B. T., Berkowitz, C. M., Kuster, W. C., Goldan, P. D., Williams, E. J., Fesenfeld, F. C., et al. (2004). Hydrocarbon source signatures in Houston, Texas: Influence of the petrochemical industry. *Journal of Geophysical Research*, 109(D24), D24305. <https://doi.org/10.1029/2004JD004887>
- Keller, C. A., Evans, M. J., Knowland, K. E., Hasenkopf, C. A., Modekurty, S., Lucchesi, R. A., et al. (2021). Global impact of COVID-19 restrictions on the surface concentrations of nitrogen dioxide and ozone. *Atmospheric Chemistry and Physics*, 21(5), 3555–3592. <https://doi.org/10.5194/acp-21-3555-2021>
- Kemball-Cook, S., Bar-Ilan, A., Grant, J., Parker, L., Jung, J., Santamaria, W., et al. (2010). Ozone impacts of natural gas development in the Haynesville shale. *Environmental Science & Technology*, 44(24), 9357–9363. <https://doi.org/10.1021/es1021137>
- Kim, S.-W., McKeen, S. A., Frost, G. J., Lee, S.-H., Trainer, M., Richter, A., et al. (2011). Evaluations of NO_x and highly reactive VOC emission inventories in Texas and their implications for ozone plume simulations during the Texas Air Quality Study 2006. *Atmospheric Chemistry and Physics*, 11(22), 11361–11386. <https://doi.org/10.5194/acp-11-11361-2011>
- Lamsal, L. N., Duncan, B. N., Yoshida, Y., Krotkov, N. A., Pickering, K. E., Streets, D. G., & Lu, Z. (2015). U.S. NO₂ trends (2005–2013): EPA air quality system (AQS) data versus improved observations from the ozone monitoring instrument (OMI). *Atmospheric Environment*, 110, 130–143. <https://doi.org/10.1016/j.atmosenv.2015.03.055>
- Lamsal, L. N., Krotkov, N. A., Celarier, E. A., Swartz, W. H., Pickering, K. E., Bucsela, E. J., et al. (2014). Evaluation of OMI operational standard NO₂ column retrievals using in situ and surface-based NO₂ observations. *Atmospheric Chemistry and Physics*, 14(21), 11587–11609. <https://doi.org/10.5194/acp-14-11587-2014>
- Lamsal, L. N., Krotkov, N. A., Vasilkov, A., Marchenko, S., Qin, W., Yang, E.-S., et al. (2021). Ozone Monitoring Instrument (OMI) Aura nitrogen dioxide standard product version 4.0 with improved surface and cloud treatments. *Atmospheric Measurement Techniques*, 14(1), 455–479. <https://doi.org/10.5194/amt-14-455-2021>
- Lamsal, L. N., Martin, R. V., Donkelaar, A., Steinbacher, M., Celarier, E. A., Bucsela, E., et al. (2008). Ground-level nitrogen dioxide concentrations inferred from the satellite-borne Ozone Monitoring Instrument. *Journal of Geophysical Research*, 113(D16), D16308. <https://doi.org/10.1029/2007JD009235>
- Laughner, J. L., Neu, J. L., Schimel, D., Wennberg, P. O., Barsanti, K., Bowman, K. W., et al. (2021). Societal shifts due to Covid-19 reveal large-scale complexities and feedbacks between atmospheric chemistry and climate change. *Proceedings of the National Academy of Sciences of the United States of America*, 118(46), e2109481118. <https://doi.org/10.1073/pnas.2109481118>
- Lelieveld, J., Dentener, F. J., Peters, W., & Krol, M. C. (2004). On the role of hydroxyl radicals in the self-cleansing capacity of the troposphere. *Atmospheric Chemistry and Physics*, 4(9/10), 2337–2344. <https://doi.org/10.5194/acp-4-2337-2004>
- Leuchner, M., & Rappenglück, B. (2010). VOC source–receptor relationships in Houston during TexAQS-II. *Atmospheric Environment*, 44(33), 4056–4067. <https://doi.org/10.1016/j.atmosenv.2009.02.029>
- Levelt, P. F., Hilsenrath, E., Leppelmeier, G. W., vandenOord, G. H. J., Bhartia, P. K., Tamminen, J., et al. (2006). Science objectives of the ozone monitoring instrument. *IEEE Transactions on Geoscience and Remote Sensing*, 44(5), 1199–1208. <https://doi.org/10.1109/TGRS.2006.872336>
- Levelt, P. F., Joiner, J., Tamminen, J., Veefkind, J. P., Bhartia, P. K., Stein Zweers, D. C., et al. (2018). The ozone monitoring instrument: Overview of 14 years in space. *Atmospheric Chemistry and Physics*, 18(8), 5699–5745. <https://doi.org/10.5194/acp-18-5699-2018>
- Limón, E. (2020). Here's how the COVID-19 pandemic has unfolded in Texas since March. Retrieved from <https://www.texastribune.org/2020/07/31/coronavirus-timeline-texas/>
- Liu, F., Page, A., Strode, S. A., Yoshida, Y., Choi, S., Zheng, B., et al. (2020). Abrupt decline in tropospheric nitrogen dioxide over China after the outbreak of COVID-19. *Science Advances*, 6(28), eabc2992. <https://doi.org/10.1126/sciadv.abc2992>
- Lyon, D. R., Hmiel, B., Gautam, R., Omara, M., Roberts, K. A., Barkley, Z. R., et al. (2021). Concurrent variation in oil and gas methane emissions and oil price during the COVID-19 pandemic. *Atmospheric Chemistry and Physics*, 21(9), 6605–6626. <https://doi.org/10.5194/acp-21-6605-2021>
- Macey, G. P., Breech, R., Cherniak, M., Cox, C., Larson, D., Thomas, D., & Carpenter, D. O. (2014). Air concentrations of volatile compounds near oil and gas production: A community-based exploratory study. *Environmental Health*, 13(1), 82. <https://doi.org/10.1186/1476-069X-13-82>
- Majid, A., Val Martin, M., Lamsal, L. N., & Duncan, B. N. (2017). A decade of changes in nitrogen oxides over regions of oil and natural gas activity in the United States. *Elementa: Science of the Anthropocene*, 5, 76. <https://doi.org/10.1525/elementa.259>
- Marchenko, S., Krotkov, N. A., Lamsal, L. N., Celarier, E. A., Swartz, W. H., & Bucsela, E. J. (2015). Revising the slant column density retrieval of nitrogen dioxide observed by the Ozone Monitoring Instrument. *Journal of Geophysical Research: Atmospheres*, 120(11), 5670–5692. <https://doi.org/10.1002/2014JD022913>
- McDonald, B. C., de Gouw, J. A., Gilman, J. B., Jathar, S. H., Akherati, A., Cappa, C. D., et al. (2018). Volatile chemical products emerging as largest petrochemical source of urban organic emissions. *Science*, 359(6377), 760–764. <https://doi.org/10.1126/science.aag0524>
- McKenna (2020). Super-polluting methane emissions twice federal estimates in Permian Basin, study finds. Retrieved from <https://insideclimatenews.org/news/22042020/permian-basin-methane-emissions-texas-new-mexico/>
- Mills, N. L., Donaldson, K., Hadoke, P. W., Boon, N. A., MacNee, W., Cassee, F. R., et al. (2009). Adverse cardiovascular effects of air pollution. *Nature Clinical Practice Cardiovascular Medicine*, 6(1), 36–44. <https://doi.org/10.1038/npcardio1399>

- Navarro-González, R., McKay, C. P., & Mvondo, D. N. (2001). A possible nitrogen crisis for Archaeal life due to reduced nitrogen fixation by lightning. *Nature*, 412(6842), 61–64. <https://doi.org/10.1038/35083537>
- Newsroom, T. T. (2021). How we got here: A timeline of gov. Greg Abbott's COVID policies. Retrieved from <https://www.houstonpublicmedia.org/articles/news/politics/2021/08/20/406474/how-we-got-here-a-timeline-of-gov-greg-abbotts-covid-policies/>
- Nowlan, C. R., Liu, X., Janz, S. J., Kowalewski, M. G., Chance, K., Follette-Cook, M. B., et al. (2018). Nitrogen dioxide and formaldehyde measurements from the GEOstationary Coastal and Air Pollution Events (GEO-CAPE) Airborne Simulator over Houston, Texas. *Atmospheric Measurement Techniques*, 11(11), 5941–5964. <https://doi.org/10.5194/amt-11-5941-2018>
- Pacsi, A. P., Kimura, Y., McGaughey, G., McDonald-Buller, E. C., & Allen, D. T. (2015). Regional ozone impacts of increased natural gas use in the Texas power sector and development in the Eagle Ford shale. *Environmental Science & Technology*, 49(6), 3966–3973. <https://doi.org/10.1021/es5055012>
- Parrish, D. D., Allen, D. T., Bates, T. S., Estes, M., Fehsenfeld, F. C., Feingold, G., et al. (2009). Overview of the second Texas air quality study (TexAQS II) and the Gulf of Mexico atmospheric composition and climate study (GoMACCS). *Journal of Geophysical Research*, 114(D7), D00F13. <https://doi.org/10.1029/2009JD011842>
- Platt, U., & Stutz, J. (2008). *Differential optical absorption spectroscopy: Principles and applications*. Springer.
- Roest, G. S., & Schade, G. W. (2020). Air quality measurements in the western Eagle Ford shale. *Elementa: Science of the Anthropocene*, 8, 18. <https://doi.org/10.1525/elementa.414>
- Schade, G. W., & Roest, G. (2016). Analysis of non-methane hydrocarbon data from a monitoring station affected by oil and gas development in the Eagle Ford shale, Texas. *Elementa: Science of the Anthropocene*, 4, 000096. <https://doi.org/10.12952/journal.elementa.000096>
- Schade, G. W., & Roest, G. (2018). Source apportionment of non-methane hydrocarbons, NO_x and H₂S data from a central monitoring station in the Eagle Ford shale, Texas. *Elementa: Science of the Anthropocene*, 6, 35. <https://doi.org/10.1525/elementa.289>
- Silvern, R. F., Jacob, D. J., Mickley, L. J., Sulprizio, M. P., Travis, K. R., Marais, E. A., et al. (2019). Using satellite observations of tropospheric NO₂ columns to infer long-term trends in US NO_x emissions: The importance of accounting for the free tropospheric NO₂ background. *Atmospheric Chemistry and Physics*, 19(13), 8863–8878. <https://doi.org/10.5194/acp-19-8863-2019>
- Souri, A. H., Choi, Y., Li, X., Kotsakis, A., & Jiang, X. (2016). A 15-year climatology of wind pattern impacts on surface ozone in Houston, Texas. *Atmospheric Research*, 174–175, 124–134. <https://doi.org/10.1016/j.atmosres.2016.02.007>
- Tong, D., Pan, L., Chen, W., Lamsal, L., Lee, P., Tang, Y., et al. (2016). Impact of the 2008 Global Recession on air quality over the United States: Implications for surface ozone levels from changes in NO_x emissions. *Geophysical Research Letters*, 43(17), 9280–9288. <https://doi.org/10.1002/2016GL069885>
- US EIA. (2021). U.S. Energy Information Administration—EIA—Independent statistics and analysis. Retrieved from <https://www.eia.gov/state/?sid=TX>
- US EIA. (2022). U.S. crude oil production forecast to rise in 2022 and 2023 to record-high levels. Retrieved from <https://www.eia.gov/todayinenergy/detail.php?id=51318>
- USEPA. (2017). Policy assessment for the review of the primary national ambient air quality standards for oxides of nitrogen [other policies and guidance]. Retrieved from <https://www.epa.gov/naaqs/policy-assessment-review-primary-national-ambient-air-quality-standards-oxides-nitrogen>
- USEPA. (2021). Final Rule: Additional revised air quality designations for the 2015 ozone national ambient air quality standards: El Paso county, Texas and weld county, Colorado [overviews and factsheets]. Retrieved from <https://www.epa.gov/ozone-designations/final-rule-additional-revised-air-quality-designations-2015-ozone-national>
- van Donkelaar, A., Martin, R. V., & Park, R. J. (2006). Estimating ground-level PM_{2.5} using aerosol optical depth determined from satellite remote sensing. *Journal of Geophysical Research*, 111(D21), D21201. <https://doi.org/10.1029/2005JD006996>
- Veefkind, J. P., de Haan, J. F., Brinksma, E. J., Kroon, M., & Levelt, P. F. (2006). Total ozone from the ozone monitoring instrument (OMI) using the DOAS technique. *IEEE Transactions on Geoscience and Remote Sensing*, 44(5), 1239–1244. <https://doi.org/10.1109/TGRS.2006.871204>
- Wang, X., Wu, Z., Zhang, Q., Cohen, J., & Pang, J. (2017). Impact of urbanization on regional climate and air quality in China. In I. Bouarar, X. Wang, & G. P. Brasseur (Eds.), *Air pollution in Eastern Asia: An integrated perspective* (pp. 453–476). Springer International Publishing. https://doi.org/10.1007/978-3-319-59489-7_22
- Zhang, R., Wang, Y., Smeltzer, C., Qu, H., Koshak, W., & Boersma, K. F. (2018). Comparing OMI-based and EPA AQS in situ NO₂ trends: Towards understanding surface NO_x emission changes. *Atmospheric Measurement Techniques*, 11(7), 3955–3967. <https://doi.org/10.5194/amt-11-3955-2018>